Geol. Mag. **155** (*5*), *2018, pp. 1063–1088.* © *Cambridge University Press 2017*
doi:10.1017/S0016756816001217

The tectonic evolution of the Bogda region from Late Carboniferous to Triassic time: evidence from detrital zircon U–Pb geochronology and sandstone petrography

JIALIN WANG*, CHAODONG WU*‡†, ZHUANG LI*, WEN ZHU*, TIANQI ZHOU*, JUN WU* & JUN WANG§

*Key Laboratory of Orogenic Belts and Crustal Evolution, Ministry of Education, School of Earth and Space Sciences, Peking University, Beijing, 100871, China
‡Institute of Oil & Gas, Peking University, Beijing, 100871, China
§Department of Xinjiang Exploration Project Management, Sinopec Shengli Oilfield Company, Dongying, Shandong, 257000, China

(*Received* 23 June 2016; *accepted* 7 December 2016; *first published online* 16 January 2017)

Abstract – Field-based mapping, sandstone petrology, palaeocurrent measurements and zircon cathodoluminescence images, as well as detrital zircon U–Pb geochronology were integrated to investigate the provenance of the Upper Carboniferous – Upper Triassic sedimentary rocks from the northern Bogda Mountains, and further to constrain their tectonic evolution. Variations in sandstone composition suggest that the Upper Carboniferous – Lower Triassic sediments displayed less sedimentary recycling than the Middle–Upper Triassic sediments. U–Pb isotopic dating using the LA-ICP-MS method on zircons from 12 sandstones exhibited similar zircon U–Pb age distribution patterns with major age groups at 360–320 Ma and 320–300 Ma, and with some grains giving ages of > 541 Ma, 541–360 Ma, 300–250 Ma and 250–200 Ma. Coupled with the compiled palaeocurrent data, the predominant sources were the Late Carboniferous volcanic rocks of the North Tianshan and Palaeozoic magmatic rocks of the Yili–Central Tianshan. There was also input from the Bogda Mountains in Middle–Late Triassic time. The comprehensive geological evidence indicates that the Upper Carboniferous – Lower Permian strata were probably deposited in an extensional context which was related to a rift or post-collision rather than arc-related setting. Conspicuously, the large range of U–Pb ages of the detrital zircons, increased sedimentary lithic fragments, fluvial deposits and contemporaneous Triassic zircon ages argue for a Middle–Late Triassic orogenic movement, which was considered to be the initial uplift of the Bogda Mountains.

Keywords: provenance, tectonic setting, detrital zircon, Late Carboniferous – Late Triassic, Bogda Mountains

1. Introduction

The Central Asian Orogenic Belt is the largest Phanerozoic juvenile crustal growth orogenic belt in the world, extending 7000 km from west to east, situated between the European Craton to the west, the Siberian Craton to the east, and the Tarim and North China cratons to the south (Fig. 1a; Charvet *et al*. 2011). It has a relatively long history dominated by accretion of arcs, accretionary complexes, seamounts and oceanic plateaus (e.g. Şengör, Natal'in & Burtman, 1993; Carroll *et al*. 1995; Gao *et al*. 1998; Jahn, Wu & Chen, 2000; Windley *et al*. 2007; Xiao *et al*. 2009; Wong *et al*. 2010; Han *et al*. 2011). The Tianshan lies in the southern part of the belt and contains units of ophiolites, volcanic rocks, granitoids, high-grade metamorphic rocks and sedimentary sequences (e.g. Gao *et al*. 1995, 2009; Hu *et al*. 2000; Jahn, Wu & Chen, 2000; Wong *et al*. 2010). In the eastern segment of the Tianshan, the Bogda Mountains/region (hereafter referred to as the Bogda) are situated between the Junggar Basin to the north and the Turpan Basin to the south (Fig. 1b).

The Permian–Triassic of the Bogda is of particular interest because it spans a critical transition between the continental amalgamation during Devonian–Carboniferous time (e.g. Allen, Windley & Zhang, 1993; Carroll *et al*. 1995) and the development of intracontinental orogenic reactivation in Mesozoic–Cenozoic time (e.g. Hendrix *et al*. 1992). However, the tectonic setting evolution of the transitional stage continues to be debated (Wartes, Carroll & Greene, 2002; Fang *et al*. 2006; Yang *et al*. 2012*a*; Tang *et al*. 2014). For instance, (1) the Bogda have been considered to be a Carboniferous island arc (Ma, Shu & Sun, 1997; Laurent-Charvet *et al*. 2003; Xie *et al*. 2016*a*,*b*), a rift zone during Carboniferous–Permian time (He *et al*. 1994; Gu *et al*. 2000; Wang *et al*. 2016*b*), a Carboniferous island arc superimposed by an Early Permian rift (Shu *et al*. 2005), or part of a mantle plume-related large igneous province (Xia *et al*. 2004*a*, *b*). (2) The prototype of the southern

†Author for correspondence: cdwu@pku.edu.cn

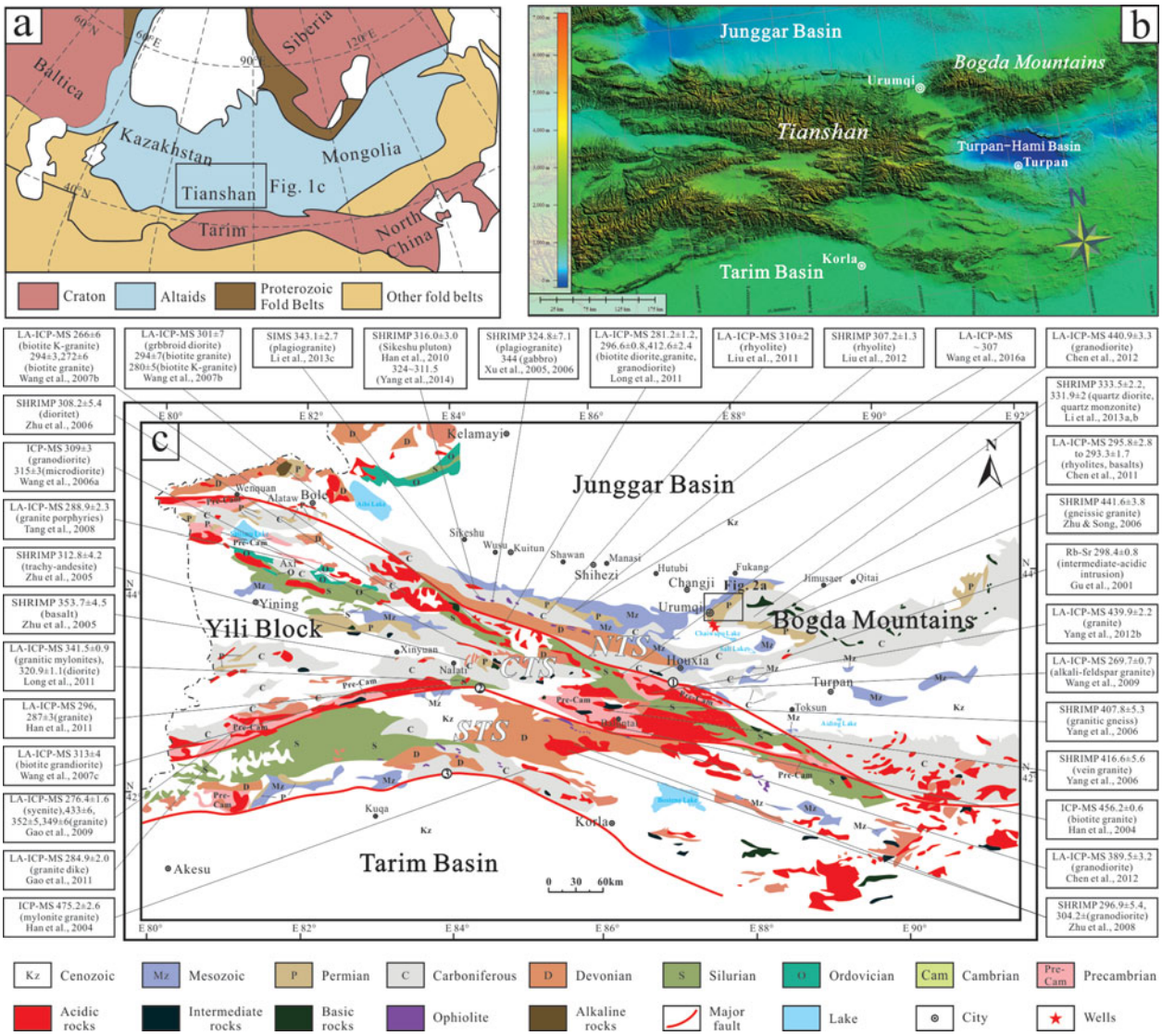

Figure 1. (Colour online) (a) Location of the Central Asian Orogenic Belt including major cratons and orogenic belts of Eurasia (modified after Wang *et al*. 2016*a*,*b*). (b) Digital topographic map of the Bogda Mountains and surrounding area. Topography from Geospatial Data Cloud. (c) Tectonic-geological sketch map of the Chinese Tianshan regions with the approximate location of Figure 2a shown with a box. The red stars represent the locations of the well core samples for zircon LA-ICP-MS U–Pb chronology analysis. The age data for igneous rocks in the NTS and adjacent tectonic units are shown in this picture. 1 – the northern margin fault of Central Tianshan; 2 – the southern margin fault of Central Tianshan; 3 – the northern Tarim margin fault; NTS – North Tianshan; CTS – Central Tianshan; STS – South Tianshan (modified from BGMRXUAR, 1993; Yang *et al*. 2012*a*; Wang *et al*. 2016*a*). The age data are from Gu *et al*. (2001), Han *et al*. (2004, 2011), Xu *et al*. (2005, 2006), Zhu *et al* (2005, 2006, 2008), Wang *et al*. (2006, 2007*b*,*c*, 2016*a*), Yang *et al*. (2006, 2012*b*, 2014), Zhu & Song (2006), Tang *et al*. (2008), Gao *et al*. (2009, 2011), Wang, Wang & Liu (2009), Chen, Shu & Santosh (2011), Liu *et al*. (2011), Long *et al*. (2011), Chen *et al*. (2012), Li *et al*. (2013*a*,*b*,*c*).

Junggar Basin in Permian time has been suggested to be a foreland basin (Hendrix *et al*. 1992; Carroll *et al*. 1995; Hendrix, 2000; Chen *et al*. 2001), a transtensional basin (Allen, Şengör & Natal'in, 1995; Cai, Chen & Jia, 2000; Chen, Wang & Wang, 2005) or a fault-controlled depression during an extensional tectonic episode (Fang *et al*. 2006; Yang *et al*. 2012*a*; Liu, Guo & Zhang, 2013; Wang *et al*. 2016*b*). (3) The initial uplift time of the Bogda has been regarded as latest Palaeozoic (Wang *et al*. 2003), Early–Middle Jurassic (Hendrix *et al*. 1992; Greene *et al*. 2001, 2005; Tang *et al*. 2014) and Late Jurassic (Zhang *et al*. 2005; Fang *et al*. 2007). And (4) the process of tectonic evolution in the Bogda from Carboniferous to Triassic time is still enigmatic (Tang *et al*. 2014 and references therein). Lots of researchers have focused on the age, nature and tectonic setting of the various tectonostratigraphic units in the Bogda (Shu *et al*. 2005; Fang *et al*. 2006; Yang *et al*. 2012*a*; Tang *et al*. 2014 and references therein), but detailed provenance analyses of these units are still lacking. Provenance analysis, as the bridge linking the sedimentary basin to orogenic belts, is one of the most important parts in reconstructing the tectonic evolution (Nie *et al*. 2012). Recent studies showed that using a combination of detrital zircon U–Pb geochronology, palaeocurrent measurement and sandstone petrography techniques can provide more reliable information on the provenance of

https://doi.org/10.1017/S0016756816001217 Published online by Cambridge University Press

Table 1. Predicted sediment provenance signatures for the NTS, YCTS and Bogda

Provenance	Detrital zircon U–Pb age spectra (Ma)	Lithofacies assemblage	Sandstone composition	Particle morphology
NTS and northern margin of YCTS	420∼360, 320∼260	Palaeozoic volcanic and volcaniclastic rocks, ophiolites	volcanic lithic and feldspar	higher proportion of euhedral grains
Southern margin of YCTS	460∼420, 410∼360, 360∼320, 300∼230	Precambrian metamorphic rocks, early Palaeozoic volcanic and granitoid rocks	quartz, volcanic and metamorphic lithic	higher proportion of rounded grains
Bogda	340∼300 (dominated by basic rocks, therefore it results in small volumes of zircons), 300∼270, 250∼200	Dominated by Carboniferous basic rocks and Palaeozoic marine–terrigenous sedimentary rocks	sedimentary lithic and quartz	mixed

Note: NTS – North Tianshan; YCTS – Yili–Central Tianshan; Bogda – Bogda Mountains/region

sedimentary rocks (e.g. Gehrels, Yin & Wang, 2003; Nie *et al*. 2012; Gehrels, 2014; Li *et al*. 2015; Li, Chen & Wei, 2016). In this contribution, we combine conventional sandstone petrography, palaeocurrent measurement and detrital zircon U–Pb geochronology to reconstruct the clastic provenance and basin–mountain interaction in the Bogda from Late Carboniferous to Late Triassic time.

2. Geological setting and potential sediment sources

Traditionally, the Tianshan is subdivided into three tectonic units: the North Tianshan (NTS), Yili–Central Tianshan (YCTS) and South Tianshan (STS) from north to south (e.g. Gao *et al*. 1998). The E–W-trending Bogda exclusively belongs to the northern part of the NTS (Fig. 1b). But considering the differences between the Bogda and the western segment of the Tianshan (NTS in this text), we describe the Bogda separately. The Tianshan results from complex accretions of island arcs and amalgamation of continental lithospheric blocks during late Palaeozoic time (Carroll *et al*. 1995; Gao *et al*. 1998; Charvet, Shu & Laurent-Charvet, 2007). The Tarim–STS and YCTS blocks collided during Devonian–Carboniferous time (e.g. Chen & Shi, 2003; Han *et al*. 2011). This accretion was followed by the collision of the newly formed Tarim–YCTS blocks with a series of the late Palaeozoic island arcs now forming the NTS (e.g. Allen, Windley & Zhang, 1993; Han *et al*. 2010; Charvet *et al*. 2011). The following summary of the Palaeozoic geological history of the Tianshan, presented in Figure 1c and Table 1, is supported by a review of isotopic ages obtained from the volcanic rocks.

2.a. The North Tianshan (NTS)

The NTS is occupied by a W–NW-striking ophiolitic mélange zone that separates the YCTS Block to the south and the Junggar Block to the north (Allen, Windley & Zhang, 1993; Gao *et al*. 1998; Han *et al*. 2010, 2011). The southward subduction of the NTS oceanic crust beneath the YCTS Block during Devonian–Carboniferous time created the Yili–NTS magmatic arc (Carroll *et al*. 1995; Gao *et al*. 1998; Wang *et al*. 2007*a*,*b*; Charvet, Shu & Laurent-Charvet, 2007). It is mainly composed of Devonian marine volcano-sedimentary rocks, and Late Carboniferous volcanic rocks and tuffs (320–300 Ma; Wang *et al*. 2016*a*), intercalated with carbonates (BGMRXUAR, 1993). The Palaeozoic structures are intruded by numerous Permian post-collisional A-type granites (300–260 Ma; Han *et al*. 2010; Chen, Shu & Santosh, 2011).

2.b. The Yili–Central Tianshan (YCTS)

The YCTS is located between the NTS and STS. The Central Tianshan and Yili are two continental units with Precambrian basements, and they are generally called the Central Tianshan Block and Yili Block (Wang *et al*. 2010*a*, 2011) or YCTS Block (Gao *et al*. 1998). The YCTS Block was mainly formed by two magmatic belts (Gao *et al*. 1998; Han *et al*. 2004). In the northern belt, the Devonian–Carboniferous arc-related volcanic rocks were generated by the NTS oceanic crust subducting southwards below the YCTS Block (420–360 and 320–300 Ma; Carroll *et al*. 1995; Gao *et al*. 1998; Wang *et al*. 2007*b*; Charvet, Shu & Laurent-Charvet, 2007; Han *et al*. 2010; Li & Peng, 2013). Post-collisional A-type granitoids have also been reported in this belt (300–260 Ma; Wang *et al*. 2007*b*). The southern magmatic belt of the YCTS is composed of Ordovician–Early Carboniferous arc-related granitic plutons produced by the northward subduction of the STS oceanic crust (460–320 Ma; Wang *et al*. 2007*a*,*c*; Gao *et al*. 2009; Han *et al*. 2011; Li & Peng, 2013).

2.c. The South Tianshan (STS)

The STS orogenic belt is bounded by the YCTS Block to the north and the Tarim Craton to the south, and is generally considered as the closure of the STS Ocean (Windley *et al*. 2007; Han *et al*. 2011). It mainly consists of Palaeozoic strata (Carroll *et al*. 1995),

https://doi.org/10.1017/S0016756816001217 Published online by Cambridge University Press

remnants of the STS oceanic lithosphere (Han *et al*. 2011), as well as active margin material of the Kazakhstan–Yili Block (Windley *et al*. 2007; Han *et al*. 2011).

2.d. The Bogda Mountains/region (Bogda)

The Bogda, located in the northern part of the NTS, contains upper Palaeozoic to Quaternary sedimentary and igneous rocks (BGMRXUAR, 1993). The upper Palaeozoic strata in the Bogda is composed mostly of Carboniferous–Early Permian bimodal volcanic rocks (340–270 Ma; Allen, Windley & Zhang, 1993; Carroll *et al*. 1995; Gao *et al*. 1998; Gu *et al*. 2000, 2001; Wartes, Carroll & Greene, 2002; Shu *et al*. 2005; Wang *et al*. 2010*b*, 2015*e*). Of these, the Carboniferous volcanic rocks are dominated by basalts (Liang *et al*. 2011), but result in minor volumes of zircons. Moreover, there are also some Triassic thin amygdaloidal andesite intercalations reported in the Jimusaer region (250–200 Ma; BGMRXUAR, 1993; Wang *et al*. 2016*b*).

2.e. The Junggar Basin

The Junggar Basin, surrounded by active mountain ranges but with little internal deformation, is one of the most prominent walled sedimentary basins in western China (Carroll, Graham & Smith, 2010). The triangle-shaped basin can be subdivided into six structural units (e.g. Qiu, Zhang & Xu, 2008). The deepest one, lying along the northern edge of the NTS, is the southern depression that has collected about 16 km of sediments since Permian time (Qiu, Zhang & Xu, 2008). The Permian magmatism in the Junggar Basin and its adjacent regions is generally attributed to an extensional tectonic setting (Ma, Shu & Sun, 1997; Jahn, Wu & Chen, 2000; Wartes, Carroll & Greene, 2002; Laurent-Charvet *et al*. 2003; Shu *et al*. 2005, 2011).

3. Stratigraphic sequences

Thick continuous marine–terrigenous sequences from the upper Palaeozoic to Mesozoic are deposited in the Bogda. A summary of the observed and published descriptions of lithology, thickness, depositional system, palaeocurrent measurements and sandstone petrography is presented (Figs 2–5).

The Carboniferous strata with a thickness of 1200–1800 m are the oldest rocks exposed in the Bogda. They are divided into two series, namely the Lower Carboniferous Qiergusitao Group (C_1qr) and the Upper Carboniferous Liushugou Formation (C_2l) and Qijiagou Formation (C_2q) (BGMRXUAR, 1999). These formations mainly consist of sandstone, mudstone, limestone, turbidite, tuff, basalt and rhyolite; the only difference is the fossil assemblages developed in these rocks (Shu *et al*. 2011). The depositional environments were interpreted as turbidite to shallow marine systems (Figs 3–5a).

The Permian strata, more than 3000 m thick, can be divided into three series. The Lower Permian defined as the Jijicaozi Group (P_1jj), which can be subdivided into the Shirenzigou Formation (P_1s) and Tashikula Formation (P_1t), is composed of sandstone, mudstone and chert intercalated with bimodal volcanic rock or alkaline basalt. The depositional environments were interpreted as shallow marine systems. The Mid Permian is further subdivided into four formations, namely the Wulapo Formation (P_2w), Jingjingzigou Formation (P_2j), Lucaogou Formation (P_2l) and Hongyanchi Formation (P_2h), which are composed of clastic rocks including conglomerate, sandstone, mudstone and oil shale. The depositional environments evolved from littoral–neritic systems in Early Permian time to delta–shallow-lacustrine systems in Middle Permian time, indicating a slight regression sequence (Figs 3, 4). The Upper Permian strata are composed entirely of non-marine sediments (Wartes, Carroll & Greene, 2002), named the Cangfanggou Group. However, despite the bad outcrop exposure, and without any precise dating ages or biostratigraphy, the Cangfanggou Group is defined as Late Permian to Early Triassic in age (Zhou *et al*. 1997).

The Cangfanggou Group (P_3–T_1ch) is transitional with the underlying strata, which is usually marked by variegated stratigraphy dominated by siliciclastic mudstone. But the lowermost strata mainly consist of red conglomerate with some argillaceous sandstone, showing characteristics of typical alluvial fan to shallow-lacustrine systems (Fig. 3, 5c; Li & Peng, 2013; Wang *et al*. 2016*b*). The Mid–Upper Triassic Xiaoquangou Group ($T_{2+3}xq$) is subdivided into three formations: the Kelamayi Formation (T_2k), Huangshanjie Formation (T_3hs) and Haojiagou Formation (T_3hj). These strata are marked by mudstone, argillaceous siltstone and sandy mudstone interbedded with conglomerate. This group was deposited in shallow-lacustrine to braided river systems (Fig. 3). The Triassic sediments are a fining-upwards depositional cycle, which reflects the increasing depth of water and expansion of the lake (Li & Peng, 2013).

4. Sampling and analytical methods

Four stratigraphic sections with a total thickness of ~4000 m were measured at a decimetre–metre scale in this study (Fig. 2). Among them, the Xiamenzi–Haxionggou section along the northern margin of the Bogda has been studied in detail because of their relatively good preservation and exposure of the Carboniferous to Triassic sedimentary series (Figs 2–4). Moreover, 12 sandstone samples ranging in age from Late Carboniferous to Late Triassic were collected from two field sections and two well cores for detrital zircon U–Pb geochronology analysis (Figs 1b, 2). Of these, six samples of the Upper Carboniferous – Upper Triassic strata were selected from the eastern Xiamenzi–Haxionggou profile (Fig. 2), two samples of the Lucaogou Formation from the western Niufengou

https://doi.org/10.1017/S0016756816001217 Published online by Cambridge University Press

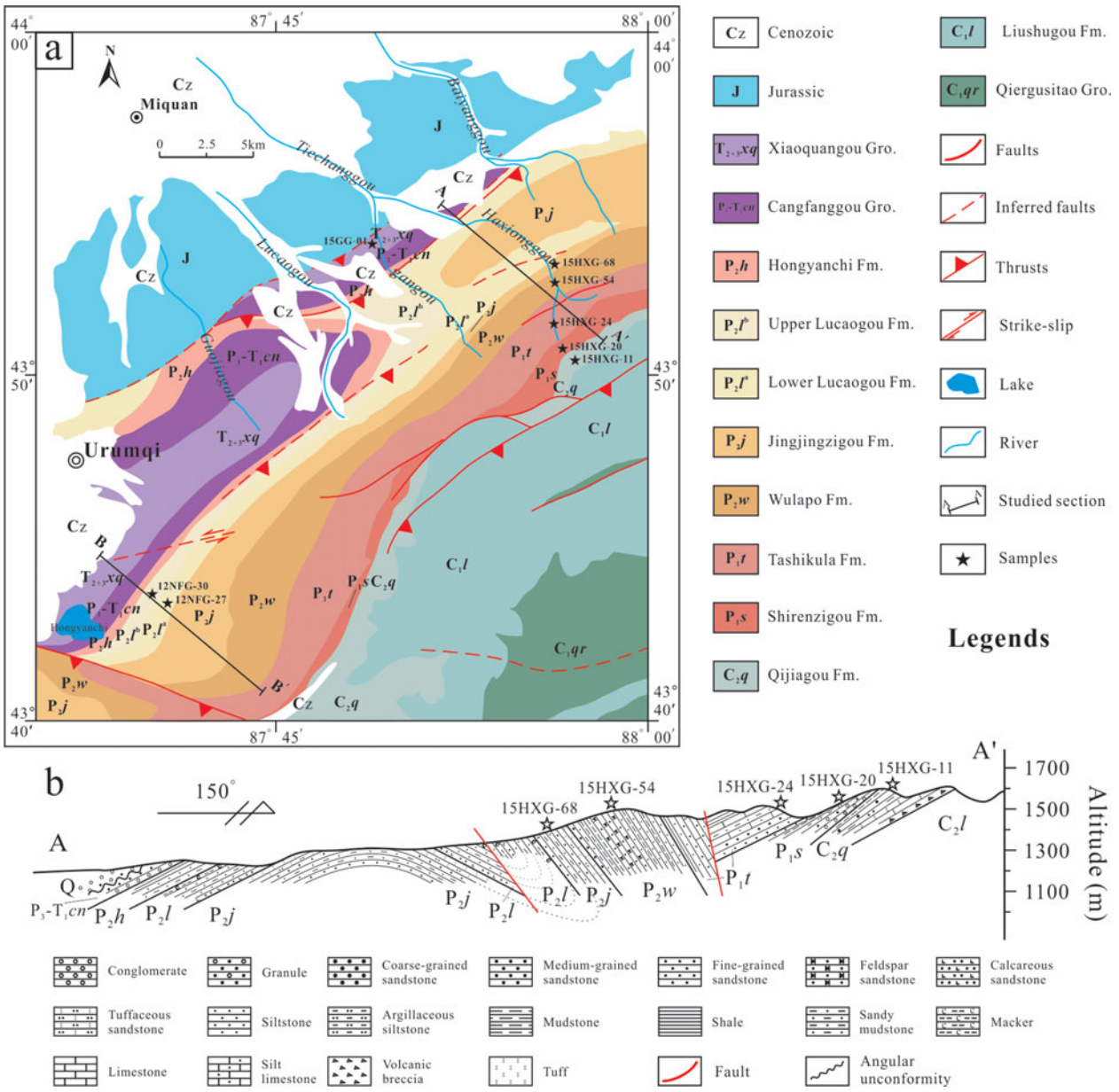

Figure 2. (Colour online) (a) Simplified geological map of the study area with the measured section of Figure 2b shown with a black line. (b) Measured section of the Upper Carboniferous to Lower Triassic strata along the Xiamenzi–Haxionggou section. The stars represent the location of the selected samples for zircon LA-ICP-MS U–Pb geochronology analysis.

profile (Fig. 2a), and four samples of the Upper Permian to Upper Triassic strata from the well cores near Urumqi (Fig. 1c). The sources of the sediments in the profiles and well cores share similar characteristics owing to their equivalent stratigraphic sequences and relatively short distances between sampling areas. The major characteristics of the samples are described in Table 2.

4.a. Sandstone petrography

Acquisition of sandstone compositional data from point-counting (systematic identification and classification of constituent minerals and lithic fragments) yields quantitative information on the contributing source lithology (Dickinson *et al*. 1983; Ingersoll *et al*. 1984). A total of 28 thin-sections were counted according to the Gazzi–Dickinson method, in which the constituent mineral directly under the cross-hairs of the petrographic microscope is identified and counted (Dickinson, 1985; Ingersoll *et al*. 1984). For each sample, at least 300 individual grains were counted and categorized. Raw data were parameterized for each sample and calculated as total quartz (Qt = monocrystalline quartz (Qm) + polycrystalline quartz (Qp)), feldspar (F = plagioclase (P) + potassium feldspar (K)), and unstable lithic fragments of sedimentary/metasedimentary (Ls) and volcanic/metavolcanic (Lv) rocks. Raw data are presented in online Supplementary Material Table S1 available at http://journals.cambridge.org/geo. Representative thin-sections are shown in Figure 5.

https://doi.org/10.1017/S0016756816001217 Published online by Cambridge University Press

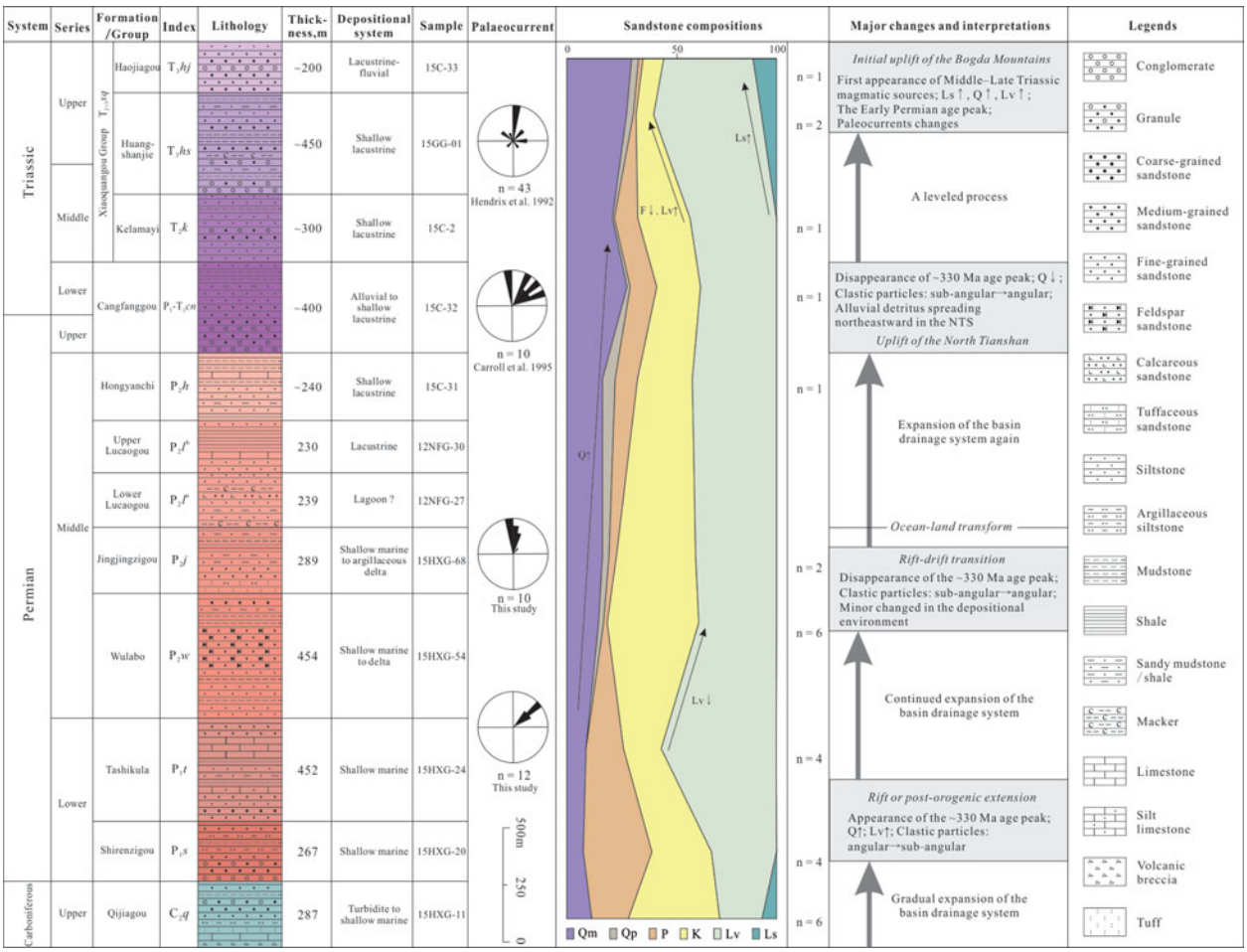

Figure 3. (Colour online) Generalized stratigraphic column of the studied Upper Carboniferous to Upper Triassic series. See text for series descriptions, depositional environments, sandstone compositions and interpretations. The published palaeocurrent data are from Hendrix *et al*. (1992) and Carroll *et al*. (1995).

Table 2. Summary of major characteristics of the sandstone samples

System	Formation/group	Sample name	Lithofacies
Upper Triassic	Haojiagou Fm	15C-33	Light-grey medium-grained sandstone
Mid–Upper Triassic	Xiaoquangou Gro	15GG-01	Taupe medium–coarse-grained sandstone
Mid Triassic	Kelamayi Fm	15C-2	Dark-red fine-grained sandstone
Upper Permian – Lower Triassic	Cangfanggou Gro	15C-32	Grey-green medium–coarse-grained sandstone
Mid Permian	Hongyanchi Fm	15C-31	Brown-red medium-grained sandstone
Mid Permian	Upper Lucaogou Fm	12NFG-30	Dark-grey fine-grained sandstone
Mid Permian	Lower Lucaogou Fm	12NFG-27	Taupe medium-grained sandstone
Mid Permian	Jingjingzigou Fm	15HXG-68	Grey-white medium-grained sandstone
Mid Permian	Wulapo Fm	15HXG-54	Grey-white medium–coarse-grained sandstone
Lower Permian	Tashikula Fm	15HXG-24	Grey-green medium–coarse-grained sandstone
Lower Permian	Shirenzigou Fm	15HXG-20	Grey-green fine-grained sandstone
Upper Carboniferous	Qijiagou Fm	15HXG-11	Grey medium-grained sandstone

4.b. Detrital zircon U–Pb geochronology

Crustal rocks generally contain zircons resistant to chemical weathering and post-depositional diagenetic processes (Nie *et al*. 2012 and references therein). In cases where possible sources exhibit diagnostic zircon U–Pb age distribution patterns, one can infer the original source by dating zircons from the basin fill (Nie *et al*. 2012). Zircon grains were dated by the laser ablation-inductively coupled plasma-mass spectrometry (LA-ICP-MS) method. Zircon grains were extracted using heavy liquid and magnetic methods, and further purified by hand-picking under a binocular microscope. Zircons were set in an epoxy mount, which was polished and then vacuum-coated with a layer of 50 nm high-purity gold. Cathodoluminescence (CL) images of the zircons were used to examine the internal structure of individual grains. CL images of representative zircon grains are presented in online Supplementary Material Figure S1 available at http://journals.cambridge.org/geo. LA-ICP-MS U–Pb zircon dating of the 12 samples was performed with an

https://doi.org/10.1017/S0016756816001217 Published online by Cambridge University Press

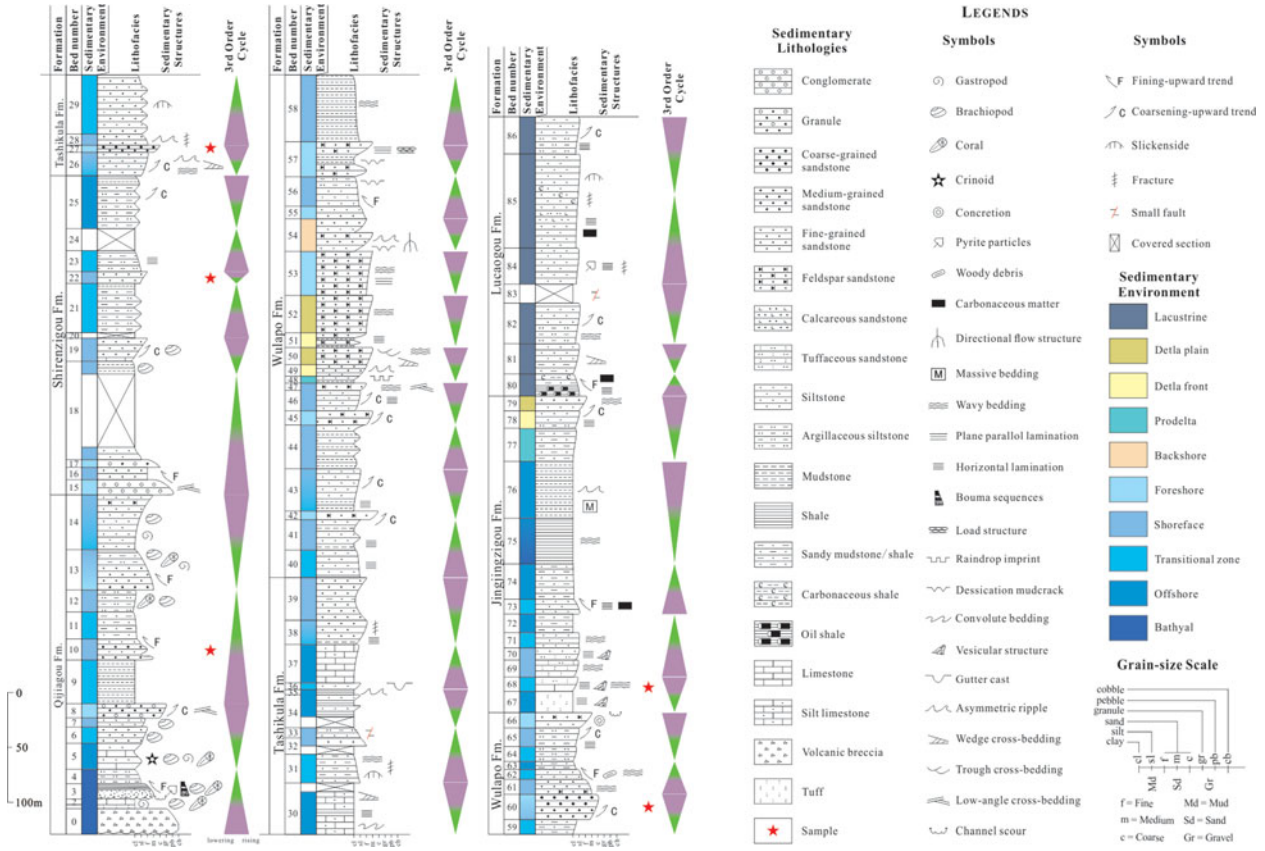

Figure 4. (Colour online) Detailed measured sections from the Upper Carboniferous Qijiagou Formation to Mid Permian Lucaogou Formation at the Xiamenzi–Haxionggou section, northern Bogda Mountains (see Figs 1b, 2 for locations).

Agilent 7500c ICP-MS equipped with a 193 nm laser (COMPexPro102) at the Key Laboratory of Orogenic Belts and Crustal Evolution, Ministry of Education, School of Earth and Space Sciences, Peking University. The detailed analysis procedures are similar to those described by Yuan *et al*. (2004) and Li & Chen (2014). The spot diameter was 32 μm. Zircon 91500 was used as an external standard age calibration, the standard glass NIST 610 was used to optimize the machine and zircon Plesovice was used as a monitoring standard. $^{207}Pb/^{206}Pb$, $^{206}Pb/^{238}U$ and $^{207}Pb/^{235}U$ ratios and apparent ages were calculated using the GLITTER 4.0 program (Jackson *et al*. 2004). Measured compositions were corrected to common Pb using the measured non-radiogenic ^{204}Pb (Andersen, 2002). The age calculations and plotting of concordia diagrams were done by ISOPLOT 3.0 with uncertainties quoted at the 1σ standard deviation and 95 % confidence levels (Ludwig, 2003). The analytical data are given in online Supplementary Material Table S2 available at http://journals.cambridge.org/geo.

For usual U–Pb (LA-ICP-MS) dating of detrital zircons, approximately 80–120 grains for each sample need to meet the requirements for statistical analysis of a basic age distribution (Andersen, 2005). In this study, 90–100 grains from each sample were selected randomly for analysis, so the results should reflect the provenance characteristics. Ages with a discordance degree of > 10 % were excluded from the analysis (Gehrels, Yin & Wang, 2003; Gehrels, 2014).

5. Results

5.a. Sandstone petrography

Raw point-count data were recalculated into detrital modes following the methods of Dickinson (1985) and plotted on Qt–F–L and Qm–F–Lt ternary diagrams (Fig. 6; Dickinson, 1985). The sandstones from all samples in this study are lithic-rich (mean $Qm_{16}F_{42}Lt_{42}$). They contain a large proportion of lithic volcanic grains, attesting to a dominantly volcanic provenance (Figs 3, 6). The trends in framework grain composition discussed below are derived from a subset of 28 thin-sections collected from the Xiamenzi–Haxionggou section, Niufengou section and well cores.

5.a.1. Quartz and feldspar grains

Quartz grain abundance increases steadily upwards from the Upper Carboniferous to Upper Triassic, balanced by a concurrent decrease in feldspar grains (Fig. 3). However, the sum of all types of quartz grains displays a slightly more pronounced decrease through the Mid Triassic Kelamayi Formation,

https://doi.org/10.1017/S0016756816001217 Published online by Cambridge University Press

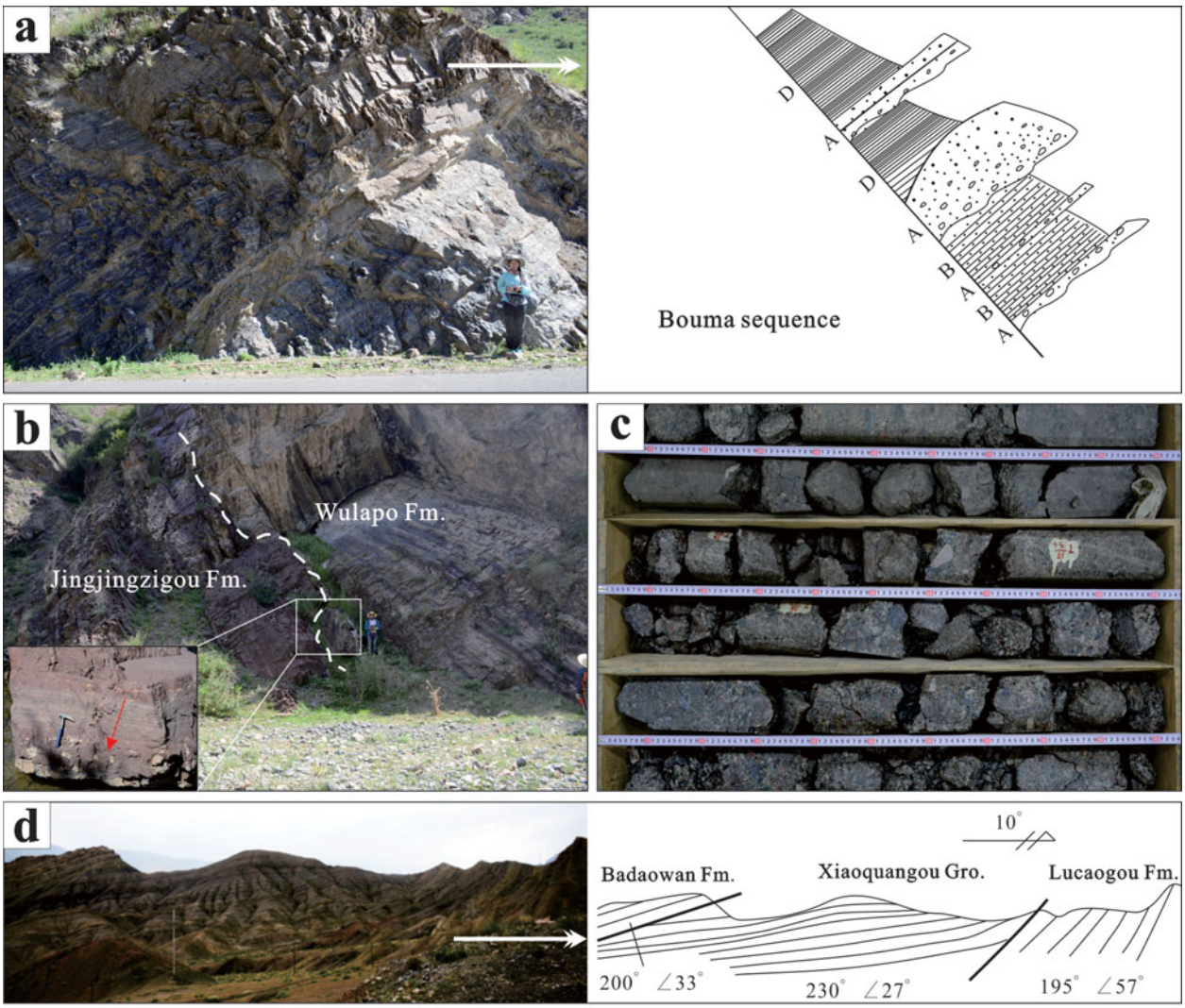

Figure 5. (Colour online) (a) Bouma sequence, including the A unit (graded bedding conglomerate), B unit (parallel bedding sandstone) and D unit (horizontal lamination); Qijiagou Formation, person (for scale) is 1.6 m tall. (b) An erosional contact (dashed line) which was caused by a relative sea-level fluctuation separating the Jingjingzigou Formation from the overlying Wulapo Formation; person (for scale) is 1.7 m tall. (c) Matrix-supported conglomerate, clasts are very poorly sorted, lack preferred orientation and a vertical grain-size trend; alluvial fan deposits of the Cangfanggou Group from the well core observation. (d) The angular unconformity contact between the Badaowan Formation, Xiaoquangou Group and Lucaogou Formation; sites were in the Aiweiergou area, Houxia; telegraph pole is 10 m high. (e–j) Photomicrographs of the sandstone samples under cross-polarized light; see text for details. Abbreviation of minerals: Cc – calcite; F – feldspar; K – potassium feldspar; Lv – volcanic/metavolcanic lithic fragment; Ls – sedimentary/metasedimentary lithic fragment; P – plagioclase; Qm – monocrystalline quartz; Qp – polycrystalline quartz.

because of a slight increase in the abundance of lithic grains (Fig. 3). From the Mid Permian Tashikula Formation to the Jingjingzigou Formation, the K grains increase from 18 % to 38 % (online Supplementary Material Table S1 available at http://journals.cambridge.org/geo), which could be evidence of increasing exposure of granitoids.

5.a.2. Lithic grains

The lithic grains are dominated by Lv grains with minor Ls grains, and the relative percentage of various lithic grain types shows the dramatic changes through time (Fig. 3). In the Upper Carboniferous samples, Lv and Ls (mainly bioclastic) fragments compose 28 % of the framework grains. The Lv grains, mainly composed of intermediate–acid rocks, increase from the Upper Carboniferous to Lower Permian, reaching values of 56 % in the Lower Permian Tashikula Formation. The percentage of Lv grains remains unchanged throughout the Mid–Upper Permian (40~46 %). Both the Lv grains and, to a lesser extent, Ls grains increase from the Mid–Upper Triassic samples (Fig. 2). In contrast, the percentage of F grains decreases. F, Lv and Ls grain percentages for the Mid Triassic Kelamayi Formation are 37 %, 41 % and 0 %, respectively, and 10 %, 52 % and 7 %, respectively for the Mid–Upper Triassic Xiaoquangou Group.

In summary, the Lv grains dominate in the Upper Carboniferous through Lower Triassic sandstones, but a pronounced increase in Ls grains occurs in the Mid–Upper Triassic samples (Fig. 3). The most

https://doi.org/10.1017/S0016756816001217 Published online by Cambridge University Press

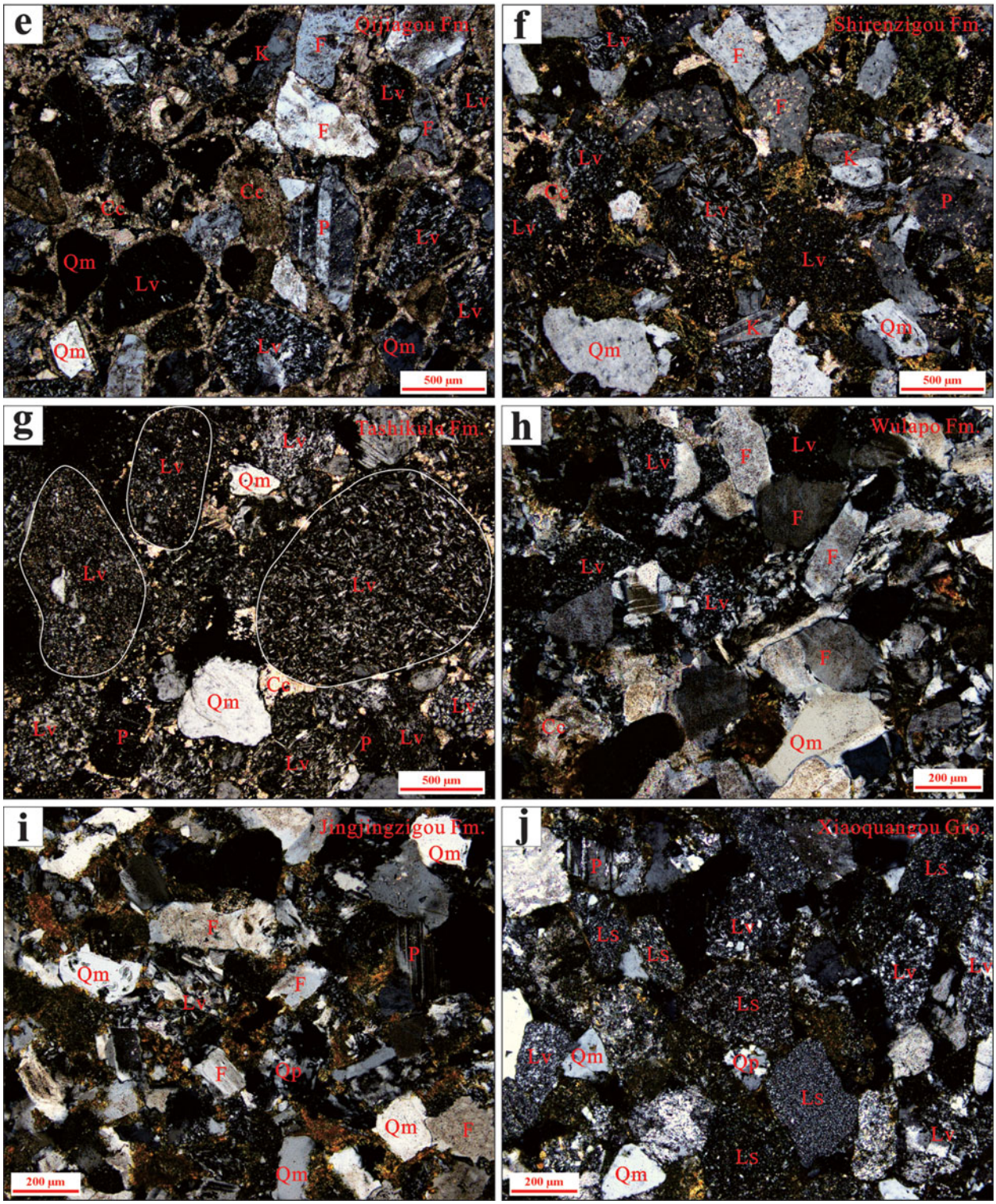

Figure 5. (Colour online) (Continued)

common Ls types are mudstone and sandstone containing some mica flakes (Fig. 5j). Furthermore, the percentage of Lv grains remains high throughout the Permian–Triassic strata, but an apparent decrease from the Tashikula to Wulapo Formation can be clearly observed (Fig. 3).

5.b. Detrital zircon U–Pb geochronology

The various zircon age groups and corresponding statistical data for the samples are shown in Table 3. Results for each sample are potted as relative age U–Pb concordia and probability density diagrams

https://doi.org/10.1017/S0016756816001217 Published online by Cambridge University Press

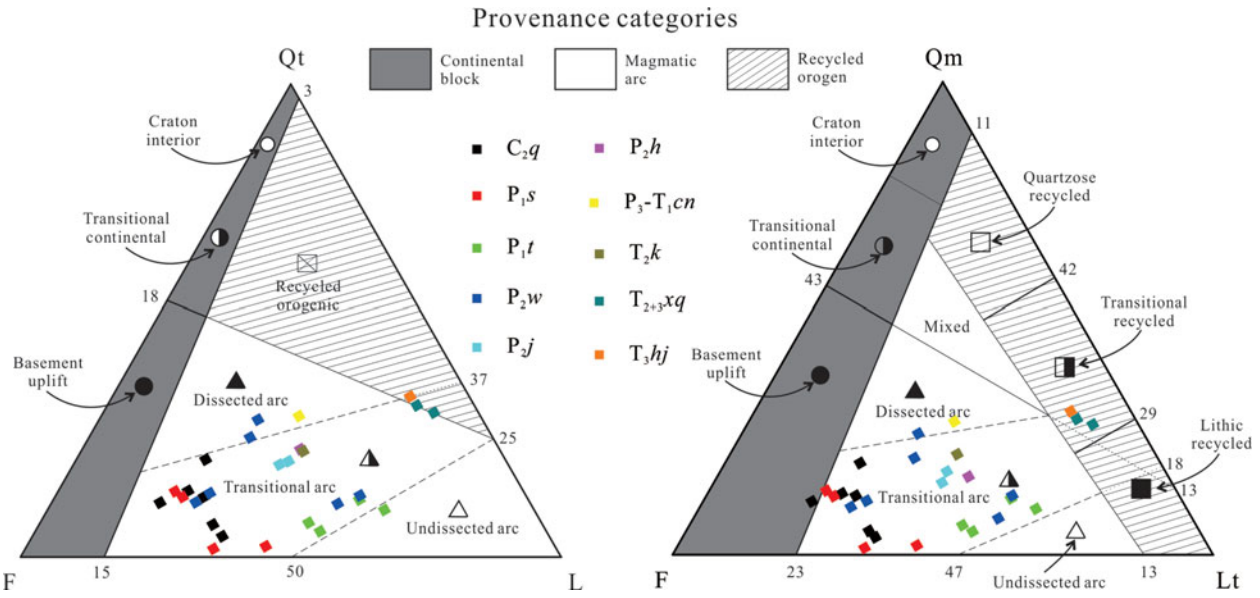

Figure 6. (Colour online) Relationship between framework composition and tectonic setting (after Dickinson, 1985). The Upper Carboniferous to Upper Triassic sandstone compositional data were plotted on the Qt–F–L and Qm–F–Lt ternary diagrams. Qt – total quartzose grains; Qm – monocrystalline quartz; Qp – polycrystalline quartz; F – total feldspar grains; P – plagioclase grains; K – potassium feldspar grains; L – unstable lithic fragments; Lt – total lithic fragments; Lv – volcanic/metavolcanic lithic fragments; Ls – sedimentary/metasedimentary lithic fragments. Qt = Qm + Qp; L = Lv + Ls; Lt = L + Qp.

(Figs 7, 8). More than 1100 U–Pb zircon analyses have been conducted for 12 samples to satisfy the statistical requirements. Almost all the zircons have subhedral to euhedral crystal shapes, a variable grain size of 50–160 μm, low luminescence and concentric oscillatory zoning (online Supplementary Material Figure S1 available at http://journals.cambridge.org/geo), with Th/U values higher than 0.1 (online Supplementary Material Table S2 available at http://journals.cambridge.org/geo), implying an igneous origin (Pupin, 1980; Corfu *et al*. 2003).

5.b.1. *Late Carboniferous samples*

A total of 91 zircon grains were measured for the Late Carboniferous sample 15HXG-11, which was collected from the Qijiagou Formation, and 90 effective data points were obtained. Ninety U–Pb analyses give a range of ^{206}Pb–^{238}U ages scattering between 352 and 277 Ma. The ^{206}Pb–^{238}U age spectrum has a major peak at 310 Ma (Fig. 8).

5.b.2. *Early Permian samples*

Sample 15HXG-20 from the Shirenzigou Formation yielded 90 effective data points with sufficient concordance and precision. The ^{206}Pb–^{238}U ages range from 868 to 284 Ma, and the ages can be divided into four groups: 300–284 Ma (21 grains); 320–301 Ma (peak at 308 Ma, 49 grains); 347–322 Ma (12 grains); and 501–362 Ma (7 grains). The oldest age, from this sample, is 868 ± 12 Ma.

Sample 15HXG-24 was collected from the Tashikula Formation. Ninety-nine U–Pb analyses give a wide range of ^{206}Pb–^{238}U ages ranging from 501 to 296 Ma. Four age populations are evident: 300–296 Ma (7 grains); 320–301 Ma (peak at 304 Ma, 55 grains); 339–321 Ma (peak at 330 Ma, 35 grains); and 501–441 Ma (2 grains).

5.b.3. *Middle Permian samples*

Sample 15HXG-54 from the Mid Permian Wulapo Formation yielded 95 age points with sufficient concordance and precision. Unlike the Early Permian samples, the U–Pb age distribution of these zircons displays a more complicated pattern. The ages can be divided into four groups: 300–287 Ma (5 grains); 320–301 Ma (peak at 306 Ma, 30 grains); 358–322 Ma (peak at 340 Ma, with a subordinate peak at 332 Ma, 44 grains); and 540–361 Ma (peak at 516 Ma, 16 grains). However, the ^{206}Pb–^{238}U age spectrum has two major peaks at 340 and 306 Ma.

Sample 15HXG-68 was collected from the Mid Permian Jingjingzigou Formation. A total of 100 analyses were randomly selected from this sample, which yielded 100 effective data points with ages from 585 to 265 Ma. Four age populations are evident: 300–265 Ma (peak at 299 Ma, with a subordinate peak at 266 Ma, 36 grains); 320–301 Ma (peak at 318 Ma, 36 grains); 359–321 Ma (peak at 346 Ma, 19 grains); and 494–361 Ma (8 grains). One zircon yielded a ^{206}Pb–^{238}U age of 585 ± 7 Ma.

Sample 12NFG-27 from the Lower Lucaogou Formation yielded 88 concordant analyses with ages from 1023 to 276 Ma. Four age groups were obtained: 299–276 Ma (peak at 293 Ma, 32 grains); 320–301 Ma (peak at 310 Ma, 34 grains); 359–321 Ma (19 grains);

https://doi.org/10.1017/S0016756816001217 Published online by Cambridge University Press

Table 3. Summary of the various age groups and corresponding statistical data for the 12 samples

Sample name	Main age groups (Ma)	Number of grains in that group	Percentage (%)	Number of effective data points
Late Carboniferous samples				
15HXG-11	277–300	11	12.2	90
	301–320	71	78.9	
	322–352	8	8.9	
Early Permian samples				
15HXG-20	284–300	21	23.3	90
	301–320	49	54.4	
	322–347	12	13.3	
	362–501	7	7.8	
	868	1	1.1	
15HXG-24	296–300	7	7.1	99
	301–320	55	55.6	
	321–339	35	35.4	
	441–501	2	2.0	
Middle Permian samples				
15HXG-54	287–300	5	5.3	95
	301–320	30	31.6	
	322–358	44	46.3	
	361–540	16	16.8	
15HXG-68	265–300	36	36.0	100
	301–320	36	36.0	
	321–359	19	19.0	
	361–494	8	8.0	
	585	1	1.0	
12NFG-27	276–299	32	36.4	88
	301–320	34	38.6	
	321–359	19	21.6	
	362–374	2	2.3	
	1023	1	1.1	
12NFG-30	266–300	35	40.2	87
	301–320	23	26.4	
	321–358	24	27.6	
	399–472	3	3.4	
	1465–2421	2	2.3	
15C-31	272–300	7	7.0	100
	301–320	46	46.0	
	321–359	44	44.0	
	369–378	2	2.0	
	1462	1	1.0	
Late Permian – Early Triassic samples				
15C-32	273–293	5	5.6	89
	303–319	29	32.6	
	321–357	52	58.4	
	361–398	3	3.4	
Middle–Late Triassic samples				
15C-2	241–245	2	2.3	87
	289–295	4	4.6	
	301–320	46	52.9	
	322–354	29	33.3	
	367–474	5	5.7	
	956	1	1.1	
15GG-01	275–300	19	19.0	100
	301–320	38	38.0	
	321–357	22	22.0	
	400–541	20	20.0	
	1020	1	1.0	
15C-33	213–250	28	28.3	99
	251–300	24	24.2	
	301–320	17	17.2	
	321–345	14	14.1	
	395–490	13	13.1	
	584–807	3	3.0	

and 374–362 Ma (2 grains). One zircon yielded a ^{206}Pb–^{238}U age of 1023 ± 14 Ma.

Sample 12NFG-30 is from the Upper Lucaogou Formation. Ninety zircon crystals were randomly selected from this sample and 87 effective data points were obtained. The ^{206}Pb–^{238}U ages range from 2421 to 266 Ma, which can be identified as four age populations: 300–266 Ma (peak at 299 Ma, 35 grains); 320–301 Ma (peak at 316 Ma, 23 grains); 358–321 Ma (peak at 330 Ma, 24 grains); and 472–399 Ma (3 grains). Two zircons yielded ages of 2421 ± 37 Ma and 1465 ± 20 Ma.

https://doi.org/10.1017/S0016756816001217 Published online by Cambridge University Press

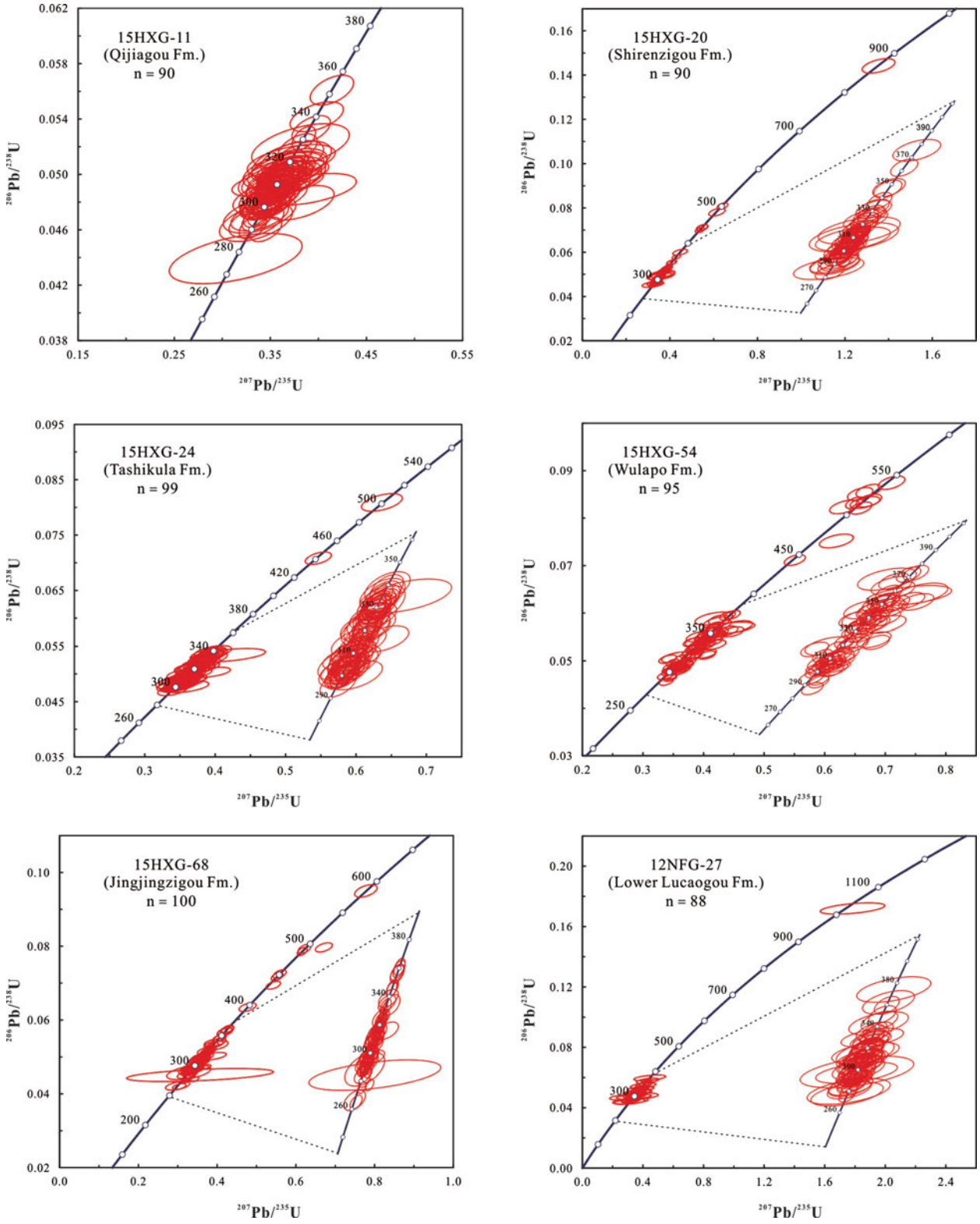

Figure 7. (Colour online) U–Pb concordia diagrams for zircon grains of the 12 sandstone samples.

Sample 15C-31 was collected from the Hongyanchi Formation in the well core near Urumqi. A total of 100 grains were analysed from this sample, which produced 100 effective data points from 1462 to 272 Ma. Four age groups are evident: 300–272 Ma (7 grains); 320–301 Ma (peak at 315 Ma; 46 grains); 359–321 Ma (peak at 330 Ma; 44 grains); and 378–369 Ma (peak at 378 Ma, 2 grains). One magmatic zircon has an age of 1462 ± 13 Ma.

5.b.4. Late Permian – Early Triassic samples

Ninety zircon crystals were randomly selected from the Late Permian – Early Triassic sample 15C-32 from

https://doi.org/10.1017/S0016756816001217 Published online by Cambridge University Press

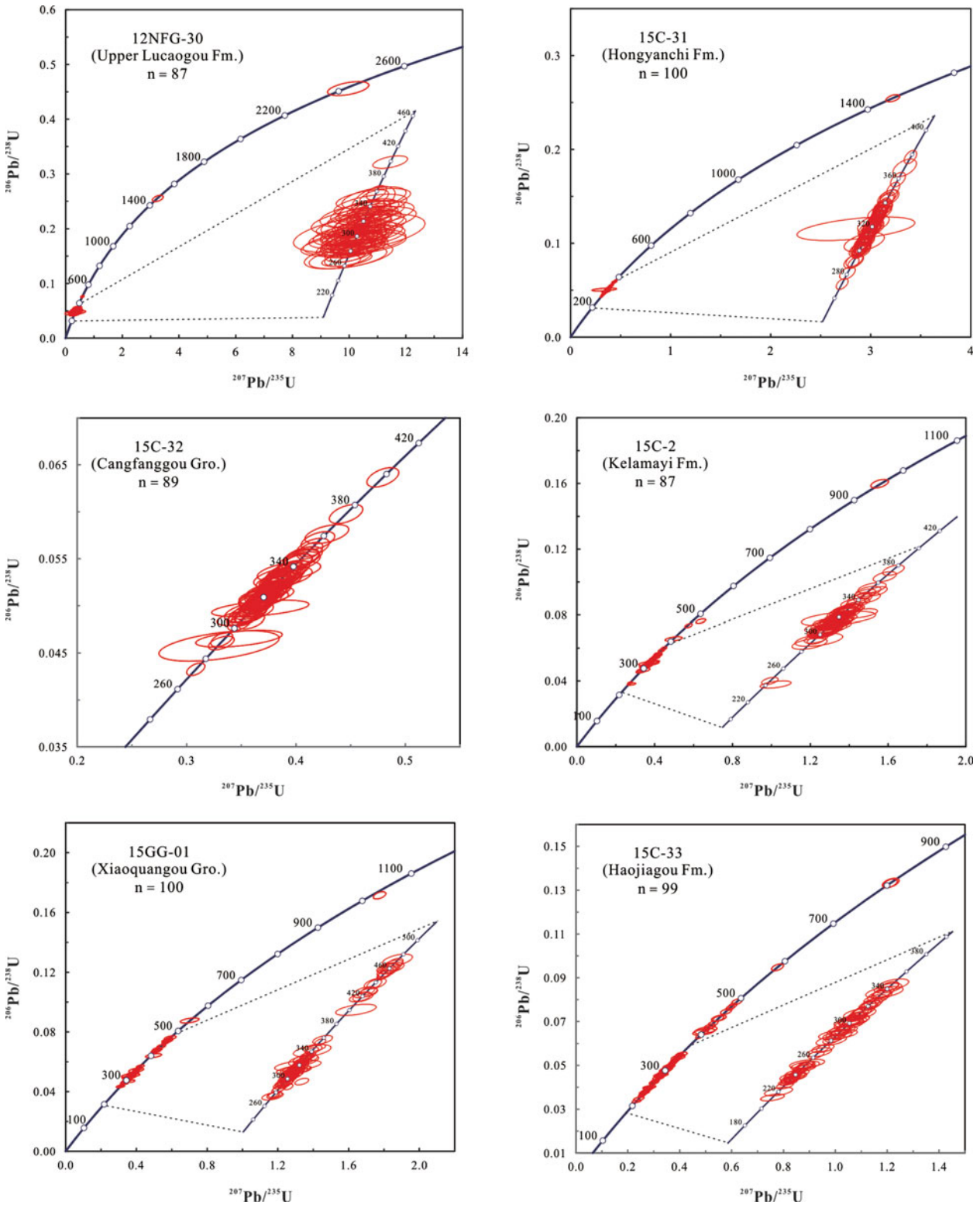

Figure 7. (Colour online) (Continued)

the well core near Urumqi and 89 effective data points were obtained. The U–Pb ages range from 398 to 273 Ma, and can be divided into four groups: 293–273 Ma (5 grains); 319–303 Ma (29 grains); 357–321 Ma (peak at 328 Ma, 52 grains); and 398–361 Ma (3 grains).

5.b.5. Middle–Late Triassic samples

Sample 15C-2 was collected from the Mid Triassic Kelamayi Formation in the well core near Urumqi. A total of 90 grains yielded 87 usable ages, which span a range from 956 to 241 Ma. Except for one

https://doi.org/10.1017/S0016756816001217 Published online by Cambridge University Press

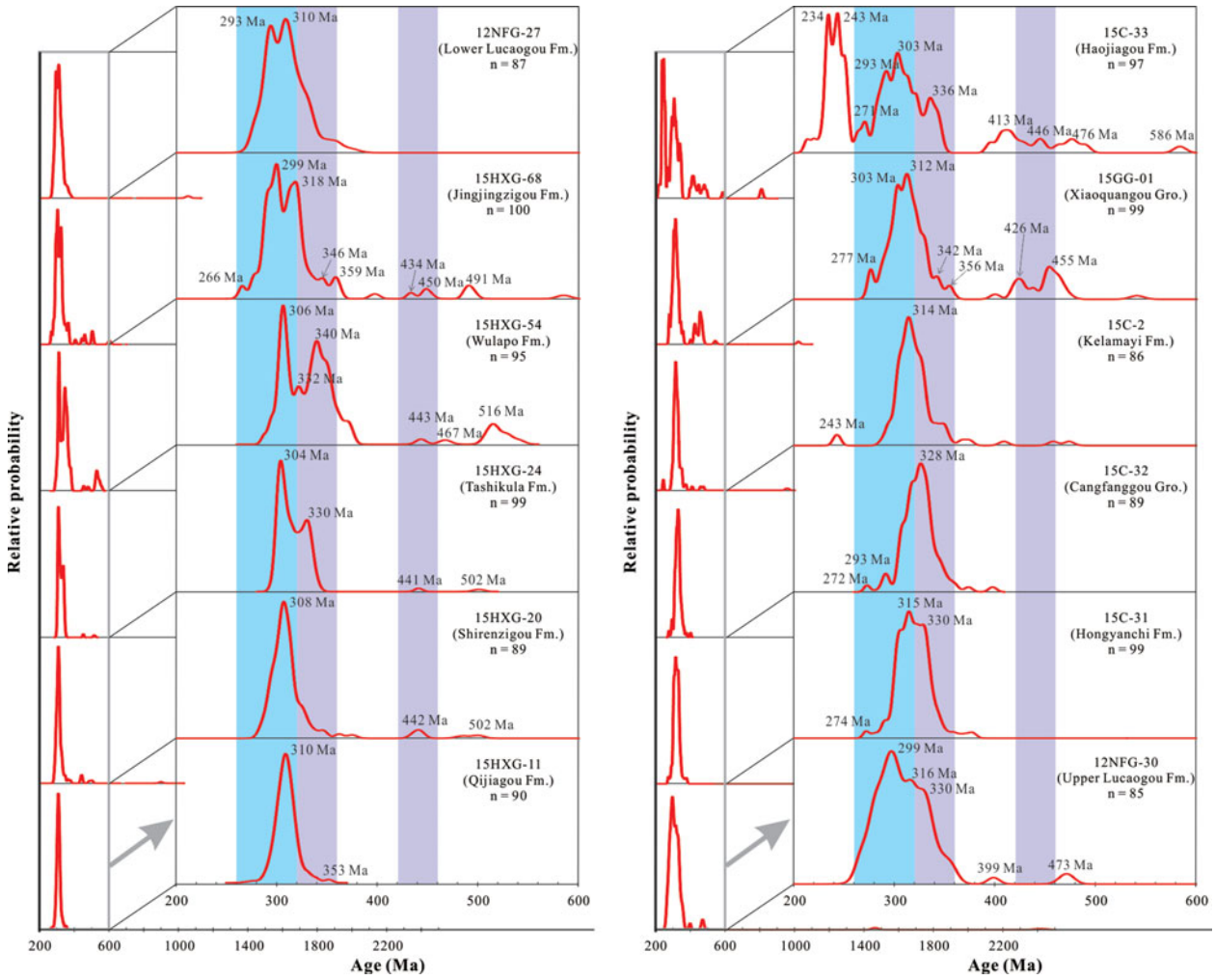

Figure 8. (Colour online) Relative U–Pb age probability plots of detrital zircons of the Upper Carboniferous to Upper Triassic sandstone samples in the Bogda Mountains.

Precambrian (956 ± 10 Ma), five Ordovician–Devonian (474–367 Ma) and two Triassic (245–241 Ma) ages, the remaining 79 zircon ages define a cluster from the Carboniferous to Early Permian (354–289 Ma), with a peak age at 314 Ma. Compared with the Cangfanggou Group, there are many more grains in the range of 320–300 Ma (more than half) and fewer grains in the range of 360–320 Ma (Fig. 9).

Sample 15GG-01 was collected from the Xiaoquangou Group in the Xiamenzi–Haxionggou section. A total of 100 analyses were conducted on these grains, which show concordant ages. The ^{206}Pb–^{238}U ages range from 1020 to 275 Ma. The results show a dominant age group of 320–301 Ma (peaks at 312 and 303 Ma, 38 grains), and subordinate groups of 300–275 Ma (peak at 277 Ma, 19 grains), 357–321 Ma (peak at 342 Ma, 22 grains) and 541–400 Ma (peaks at 455 and 426 Ma, 20 grains). One detrital zircon has an age of 1020 ± 9 Ma.

Sample 15C-33 was collected from the well core adjacent to 15C-2, 15C-31 and 15C-32. Analysis of 100 grains yielded 99 usable ages, which span a wide range from 807 to 213 Ma. Five age populations are evident: 250–213 Ma (peaks at 243 and 234 Ma, 28 grains); 300–251 Ma (peak at 293 Ma, with a subordinate peak at 271 Ma, 24 grains); 320–301 Ma (peak at 303 Ma, 17 grains); 345–321 Ma (peak at 336 Ma, 17 grains); and 490–395 Ma (peaks at 476, 446 and 413 Ma, 13 grains). Three zircons yielded ages of 807 ± 8, 806 ± 8 and 584 ± 6 Ma.

6. Discussion

6.a. Provenance

U–Pb zircon age data from the 12 analysed samples mainly fall into six groups: (1) Precambrian zircons having ages of 2421–541 Ma; (2) Cambrian to Devonian zircons ranging in age from 541 to 360 Ma; (3) Early Carboniferous zircons with ages from 360 to 320 Ma; (4) Late Carboniferous zircons with ages between 320 and 300 Ma; (5) Permian zircons having ages of 300–250 Ma; and (6) Triassic zircons with ages ranging from 250 to 200 Ma. The relative proportions of these six age components vary among samples. Palaeocurrents in the strata of the Bogda are mainly N-directed implying the provenance of the Bogda sediments was situated mainly to the south in the

https://doi.org/10.1017/S0016756816001217 Published online by Cambridge University Press

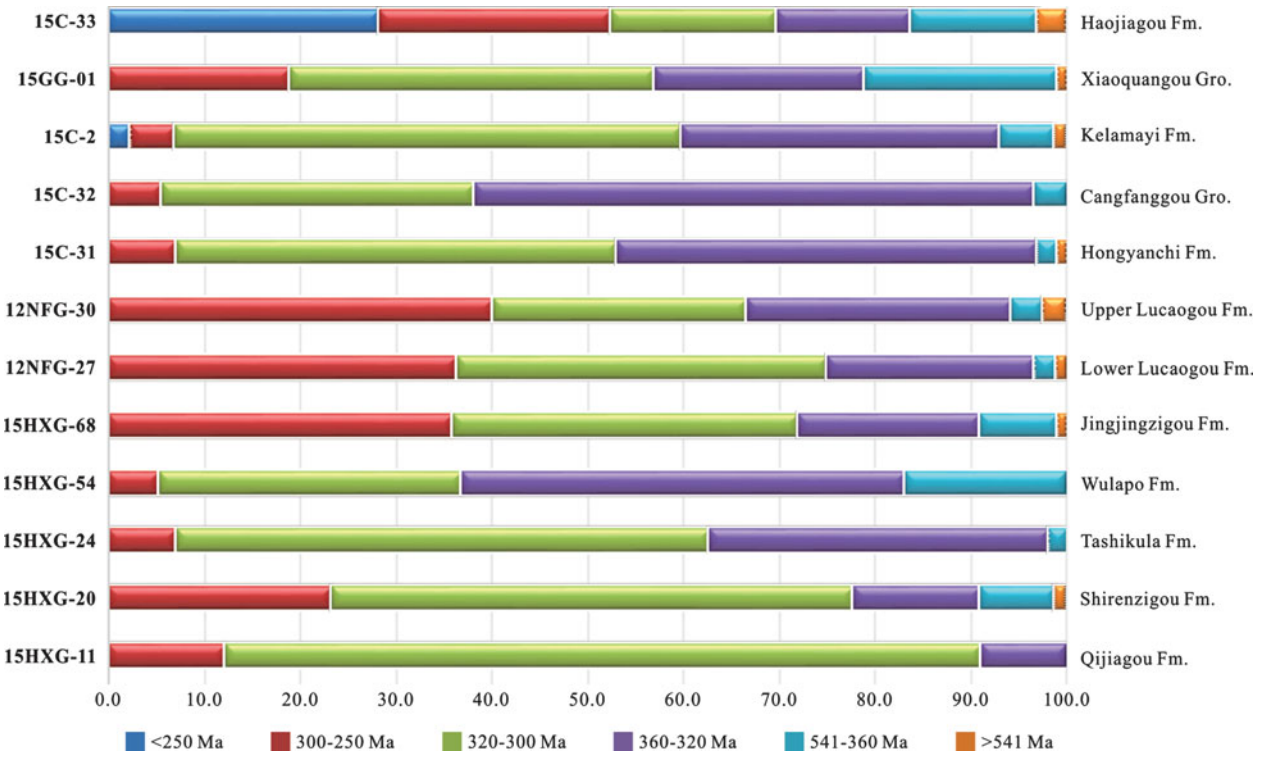

Figure 9. (Colour online) Zircon U–Pb age group variations of the 12 sandstone samples from the Upper Carboniferous Qijiagou Formation to Upper Triassic Haojiagou Formation.

Tianshan area (Hendrix *et al*. 1992; Hendrix, 2000; Greene *et al*. 2001). However, considering the long distance between the STS and the Bogda in late Palaeozoic time (Li *et al*. 2012; Li & Peng, 2013), the STS is unlikely to be the provenance of the Bogda sediments.

The age populations within 2421–541 Ma and 541–360 Ma shown in the age spectrum are consistent with the ages of the Proterozoic basement and Cambrian–Devonian magmatic rocks in the YCTS (Fig. 1c; Han *et al*. 2004; Zhu & Song, 2006; Gao *et al*. 2009; Chen *et al*. 2012; Yang *et al*. 2012*b*). Alternatively, these zircons could possibly be derived from the recycled pre-orogenic sediments. A few Devonian ages (420–360 Ma) have also been reported in the NTS and northern margin of the YCTS (Fig. 1c; Gao *et al*. 1998), but these zircons have little impact on our interpretations of detrital zircon populations (Fig. 8).

The Early Carboniferous zircons with ages from 360 to 320 Ma in the contribution correlate well with the arc-related granitic plutons produced by the northward subduction of the STS oceanic crust in the southern magmatic belt of the YCTS (Fig. 1c; Wang *et al*. 2007*a*,*c*; Gao *et al*. 2009; Han *et al*. 2011; Li & Peng, 2013), and they are the potential sources of the studied rocks. Moreover, igneous rocks with ages of 334 ± 2 Ma and 332 ± 2 Ma were also reported in the Bogda (Li *et al*. 2013*a*,*b*), but are dominated by basic rocks, therefore resulting in small volumes of zircons (Wang *et al*. 2010*b*). In summary, the 360–320 Ma zircon ages were mainly derived from the southern magmatic belt of the YCTS (Li *et al*. 2012; Li & Peng, 2013).

Detrital zircons with ages of 320–300 Ma are typically euhedral, suggesting derivation from a local source area. Our sampling area is close to the NTS. The Late Carboniferous island arc volcanic rocks are abundant in the NTS and northern margin of the YCTS, and have ages largely between 320 and 300 Ma (Table 1; Han *et al*. 2010; Liu *et al*. 2011, 2012; Yang *et al*. 2014; Wang *et al*. 2016*a*). These observations suggest that the Late Carboniferous volcanic rocks in the NTS and northern magmatic belt of YCTS were the sources.

Detrital zircons of 300–250 Ma ages have been reported in the NTS (Han *et al*. 2010), YCTS (Wang *et al*. 2007*b*; Tang *et al*. 2008; Gao *et al*. 2009, 2011; Han *et al*. 2011; Long *et al*. 2011) and the Bogda (Gu *et al*. 2001; Chen, Shu & Santosh, 2011). Thus, these zircons are unable to be unequivocally distinguished from a single region or both regions. These zircons are always from the Permian high-K calc-alkaline and alkaline igneous rocks (e.g. granites), which relate to post-collision (Liu *et al*. 2005; Shu *et al*. 2005; Chen, Shu & Santosh, 2011).

The Triassic age group (250–200 Ma) in the detrital zircons is associated with the Mesozoic magmatism, but there is relatively little direct field evidence of Triassic magmatic activity in the southern margin of the Junggar Basin. However, near the Jimusaer and slightly further east, thin amygdaloidal andesites interlayered with the Mid–Upper Triassic strata have been reported (BGMRXUAR, 1993; Wang *et al*. 2016*b*). Hence, we suggest the Bogda was probably the source of the zircons with an age range of 250–200 Ma.

https://doi.org/10.1017/S0016756816001217 Published online by Cambridge University Press

Accordingly, the provenance of the Bogda was probably derived from the NTS, YCTS and the Bogda. In spite of this, sources from the NTS and the northern margin of the YCTS would be dominated by higher proportions of euhedral and angular grains, and sandstone rich in F and Lv grains (Table 1). The source from the southern margin of the YCTS would be characterized by lower proportions of euhedral and angular grains relative to rounded grains (owing to long-distance transport and multiple-phase recycling), and sandstone rich in quartz grains with some metamorphic fragments (Table 1). The source from the Bogda would be dominated by mixed angular to rounded grains, and sandstone composed of quartz, Ls and Lv grains (Table 1).

6.b. Tectonic setting

The Late Carboniferous geodynamic setting of the NTS has long been debated (e.g. Wang *et al*. 2007*d*; Tang *et al*. 2010; Wang *et al*. 2016*a* and references therein). Fortunately, the composition of a sandstone can be related to plate tectonic processes, making it a powerful tool in the recognition of ancient tectonic settings (e.g. Dickinson, 1985). As shown in Figures 3 and 6, except for the Mid–Upper Triassic samples, the remaining sandstones plotted in the magmatic arc area, and the lithic clasts are dominated by volcanic lithic fragments. Thus, we propose that the arc-related sources were the provenance of the Upper Carboniferous – Lower Triassic sediments. As the 320–300 Ma zircon ages (mainly derived from the NTS) are always present in the age pattern of detrital zircons from the Upper Carboniferous to Lower Triassic (Figs 8, 9), we suggest the NTS was an island arc in Late Carboniferous time. This can be further evidenced by the characteristics of the volcanic rocks in the NTS (Wang *et al*. 2016*a* and references therein). The Upper Carboniferous rock assemblages of the NTS display a consecutive magma series, and most of them fall into the calc-alkaline field (Figs 10, 11; Wang *et al*. 2016*a* and references therein). On the Th–Ta–Hf/3 (Fig. 11a; Wood, 1980) and Th/Yb–Nb/Yb (Fig. 11c; Pearce, 2008) discriminant diagrams, most of the Late Carboniferous basaltic volcanic rocks plot in the calc-alkaline basalt field and reveal a subduction-related magmatism. In the Y + Nb versus Rb diagram (Pearce, 1996), the Late Carboniferous felsic volcanic rocks plot in the volcanic arc field, consistent with the characteristics of an arc-type setting of active continental margins. All of this evidence suggests that the NTS was in a subduction-related setting in Late Carboniferous time. However, in Early Permian time, the volcanic rocks show a bimodal pattern, and the granites mainly plot in the within-plate field (Fig. 11e). Some Early Permian high-K calc-alkaline and alkaline igneous rocks have also been reported (Han *et al*. 2010; Tang *et al*. 2010; Wang *et al*. 2016*a*). Therefore, we propose that the post-collisional extensional environment initiated from Early Permian time (Wang *et al*. 2016*a*).

As Section 1 mentioned, the initial tectonic setting of the Bogda is still a matter of debate. Three samples from the Mid–Upper Triassic Xiaoquangou Group plot in the recycled orogeny area instead of the magmatic arc area on the Qt–F–L and Qm–F–Lt ternary diagrams (Fig. 6). Considering the Bogda begins to provide sedimentary materials in Middle–Late Triassic time (see Section 6.c.4), we speculate that the Bogda was not a volcanic arc as proposed by Ma, Shu & Sun (1997) and Laurent-Charvet *et al*. (2003). Instead, more and more multidisciplinary data support that the Bogda was a rift in Carboniferous time (Gu *et al*. 2000, 2001; Wang *et al*. 2010*b*, 2015*e*), followed by Permian extension (Shu *et al*. 2011). This is also supported by the widely distributed Carboniferous–Early Permian bimodal volcanic rocks in the Bogda (Fig. 10; Gu *et al*. 2000; Wang *et al*. 2010*b*, 2015*e*; Chen, Shu & Santosh, 2011), the underwater olistostrome of Baiyanggou (Shu *et al*. 2011) and the regional strike-slip faults in the Tianshan (Shu *et al*. 2005). Furthermore, on the Th–Ta–Hf/3 (Fig. 11b), Th/Yb–Nb/Yb (Fig. 11d) and Rb–(Y + Nb) (Fig. 11f) discriminant diagrams, the basaltic rocks plot in multiple fields, indicating an origin from melting of variably enriched mantle sources. This evidence indicates an extensional affinity in Carboniferous–Early Permian time. Therefore, we suggest the initial tectonic setting of the Bogda was an extensional context which was related to rifting or post-collision.

6.c. Implications for tectonic evolution of the Bogda

As mentioned in Section 1, controversy has surrounded the tectonic evolution of the Tianshan, Bogda and Junggar Basin for a long time. The integrated provenance techniques employed here reveal a series of significant shifts in geochronology and sandstone composition. These variations clearly indicate that sediment sources varied in relation to four distinct stages from Late Carboniferous to Late Triassic time (Fig. 12).

6.c.1. Rift or post-collisional extension (Late Carboniferous to Early Permian)

The patterns of the detrital zircon ages from the Upper Carboniferous Qijiagou Formation (sample 15HXG-11) and Lower Permian Shirenzigou Formation (sample 15HXG-20) showed similar unimodal peaks, indicating a single source of magmatic rocks. Together with the nearly automorphic crystal fragments (e.g. feldspar and quartz) and angular detritus observed under the microscope (Fig. 5e, f), this implies that during this period the Late Carboniferous magmatic belt of the NTS and northern margin of the YCTS were the principal provenance areas. The late Early Permian sample 15HXG-24 from the Tashikula Formation showed some similarities with samples 15HXG-11 and 15HXG-20 with one major Late Carboniferous peak age. This was interpreted as again being mostly derived from the Late

https://doi.org/10.1017/S0016756816001217 Published online by Cambridge University Press

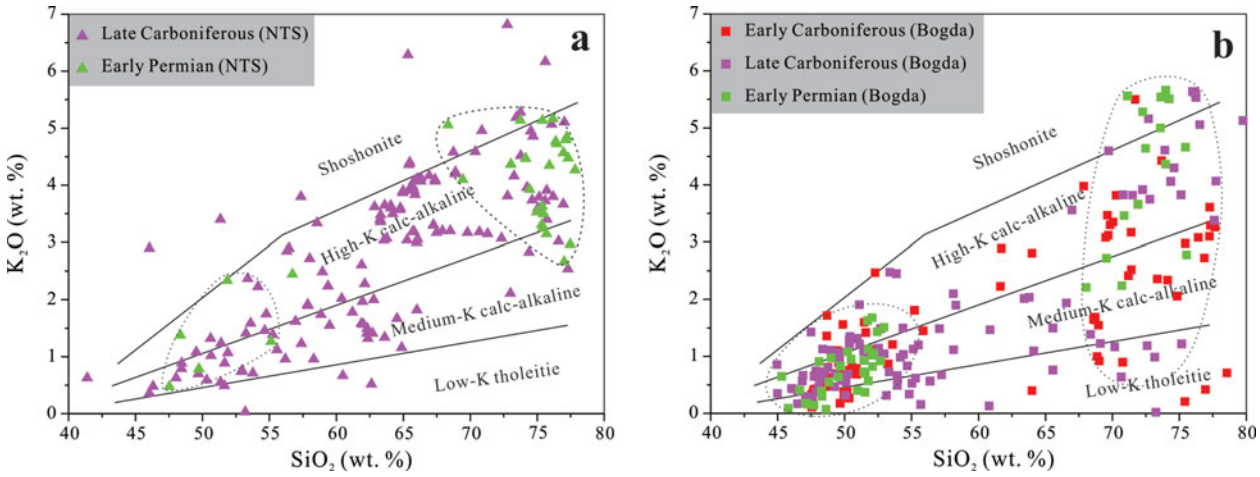

Figure 10. (Colour online) K_2O versus SiO_2 diagram for the Carboniferous – Early Permian volcanic rocks and granite–mafic intrusions in the NTS and Bogda Mountains (modified after Peccerillo & Taylor 1976). Data are from Chen *et al*. (2000, 2013), Gu *et al*. (2000, 2001), Xia *et al*. (2004*b*), Liu *et al*. (2005, 2011, 2012), Shu *et al*. (2005, 2011), Ouyang *et al*. (2006), Wang *et al*. (2007*d*, 2010*b*, 2015*a*,*b*,*c*,*d*,*e*, 2016*a*), Guo *et al*. (2009), Han *et al*. (2010), Wang & Cai (2010), Chen, Shu & Santosh (2011), Liang *et al*. (2011), Long *et al*. (2011), Xiong *et al*. (2011), Gao *et al*. (2013, 2014), Li *et al*. (2013*b*), Si *et al*. (2014), Yang *et al*. (2014), Zhao *et al*. (2014) and Xie *et al*. (2016*a*).

Carboniferous magmatic belt of the NTS and northern margin of the YCTS. However, the older peak of 330 Ma in sample 15HXG-24, associated with several early Palaeozoic ages, suggested exhumation of older and further sources that were probably derived from the southern margin of the YCTS. The appearance of the Early Carboniferous source from the southern margin of the YCTS maintained that the basin drainage widened and the distance over which sediments were transported gradually increased from Late Carboniferous to Early Permian time. This is consistent with the characteristics of the clastic particles in the thin-sections: clastic particles from the Qijiagou Formation were angular (Fig. 5e), but some of the clastic grains of the Lower Permian were sub-angular to rounded (Fig. 5f, g). All this evidence reflects the gradual expansion of the drainage systems from Late Carboniferous to Early Permian time, as well as up to Middle Permian time (see Section 6.c.2).

Taking into account the lithostratigraphic features, provenances and the published data (see Section 6.b.), the Upper Carboniferous to Lower Permian strata are interpreted as having formed possibly in an extensional context which was related to rifting or post-collision (Fig. 12a). This viewpoint had also been proposed in several previous studies (e.g. Wartes, Carroll & Greene, 2002; Shu *et al*. 2005, 2011; Fang *et al*. 2006; Wang *et al*. 2010*b*; Chen, Shu & Santosh, 2011; Yang *et al*. 2012*a*; Tang *et al*. 2014).

6.c.2. Rift-drift transition (Middle Permian)

The spectrogram of detrital zircon ages and N-directed palaeocurrents suggest that the material deposited within the Mid Permian Wulapo Formation (sample 15HXG-54) was predominantly derived from the NTS and northern margin of the YCTS (peak at 306 Ma), and minor amounts of materials were sourced from the southern margin of the YCTS (peak at 340 Ma). We propose this indicates the continued expansion of the drainage system. However, the peak age of 340 Ma disappeared in the Mid Permian Jingjingzigou Formation (sample 15HXG-68), and the clastic particles changed from sub-rounded in the Wulapo Formation (Fig. 5h) to sub-angular in the Jingjingzigou Formation (Fig. 5i). Furthermore, the minor peak age at 318 Ma in the age pattern of sample 15HXG-68 suggests older, most likely deeper sources of the NTS. Therefore, the main provenance had a shift from a mixture of two sources to a single source from the Wulapo to Jingjingzigou Formation. Although the episode of basin underfilling recorded by the Jingjingzigou Formation may reflect structural damming during local uplift of the orogenic wedge or propagation of a new frontal thrust (Lawton & Trexler, 1991; Wartes, Carroll & Greene, 2002), minor changes in depositional environment should be considered (Figs 3, 5b). Plus, the subordinate peak ages (359 Ma and 346 Ma), associated with several early Palaeozoic ages, indicate that the YCTS still provided some materials to the Bogda. That is, though the NTS source was important, positive reliefs were certainly present but were probably smooth enough to allow rivers to cut through and bring materials from the YCTS to the north. These results suggest that the main watershed did not exist between the YCTS and NTS in this period. In addition, syn-sedimentary normal faults are widely distributed in the Lower Permian strata, revealing a rift-related depositional environment (Wang *et al*. 2016*b*). In Middle Permian time, the depositional environment was relatively stable, without intensive deformation, showing weak tectonic activity (Wang *et al*. 2016*b*). These phenomena are incongruent with the local uplift model, which would cause a sharp provenance

https://doi.org/10.1017/S0016756816001217 Published online by Cambridge University Press

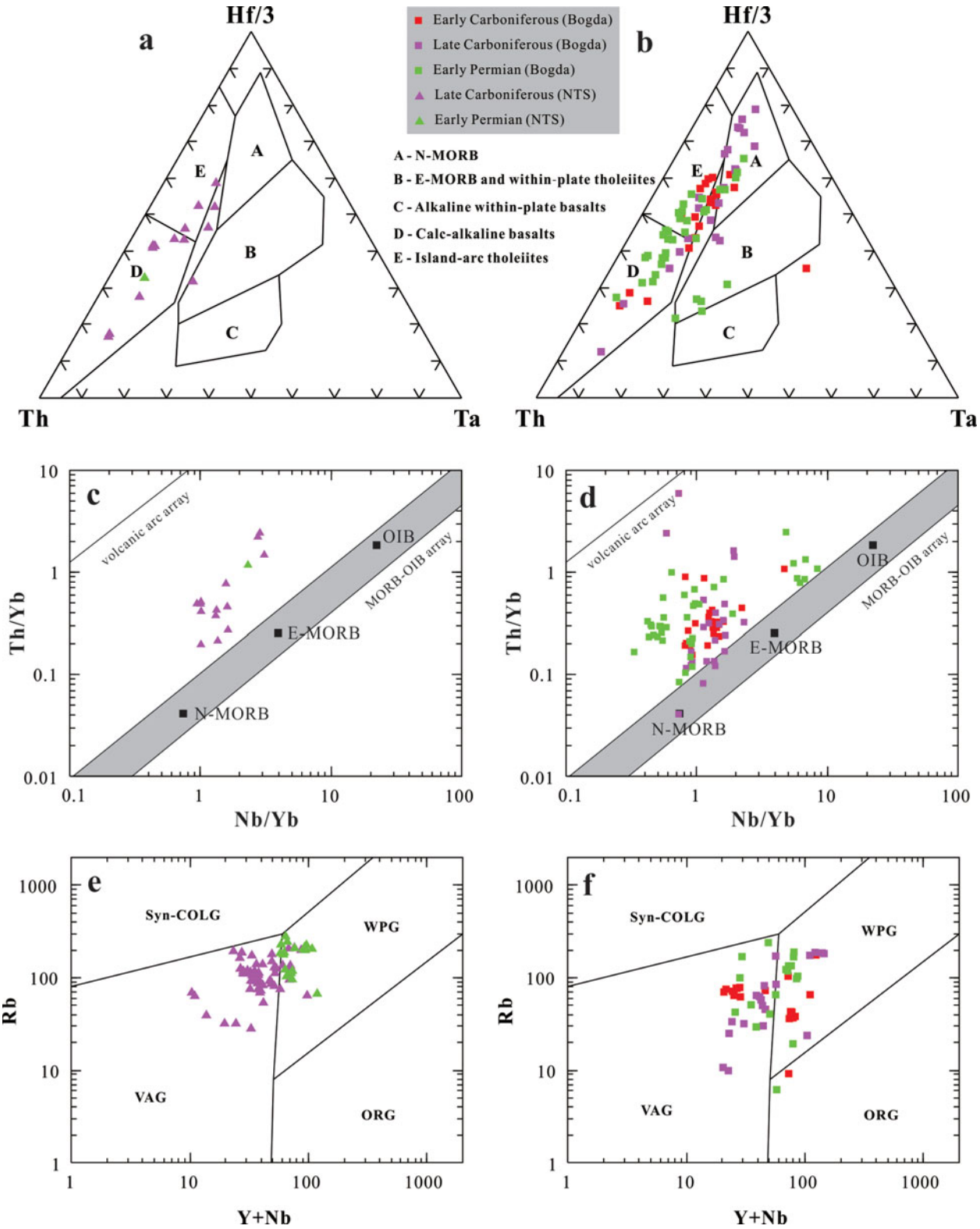

Figure 11. (Colour online) Discrimination diagrams illustrating the tectonic setting of the volcanic rocks from the Bogda Mountains and NTS. (a, b) Th–Ta–Hf/3 discriminant diagrams (basaltic only; fields after Wood, 1980); (c, d) Th/Yb versus Nb/Yb discriminant diagrams (basaltic only; fields after Pearce, 2008); (e, f) Rb versus Yb + Nb discriminant diagrams (felsic only; fields after Pearce, 1996). Data sources are the same as in Figure 10. WPG – within-plate granites; VAG – volcanic arc granites; Syn-COLG – syn-collision granites; ORG – ocean ridge granites.

https://doi.org/10.1017/S0016756816001217 Published online by Cambridge University Press

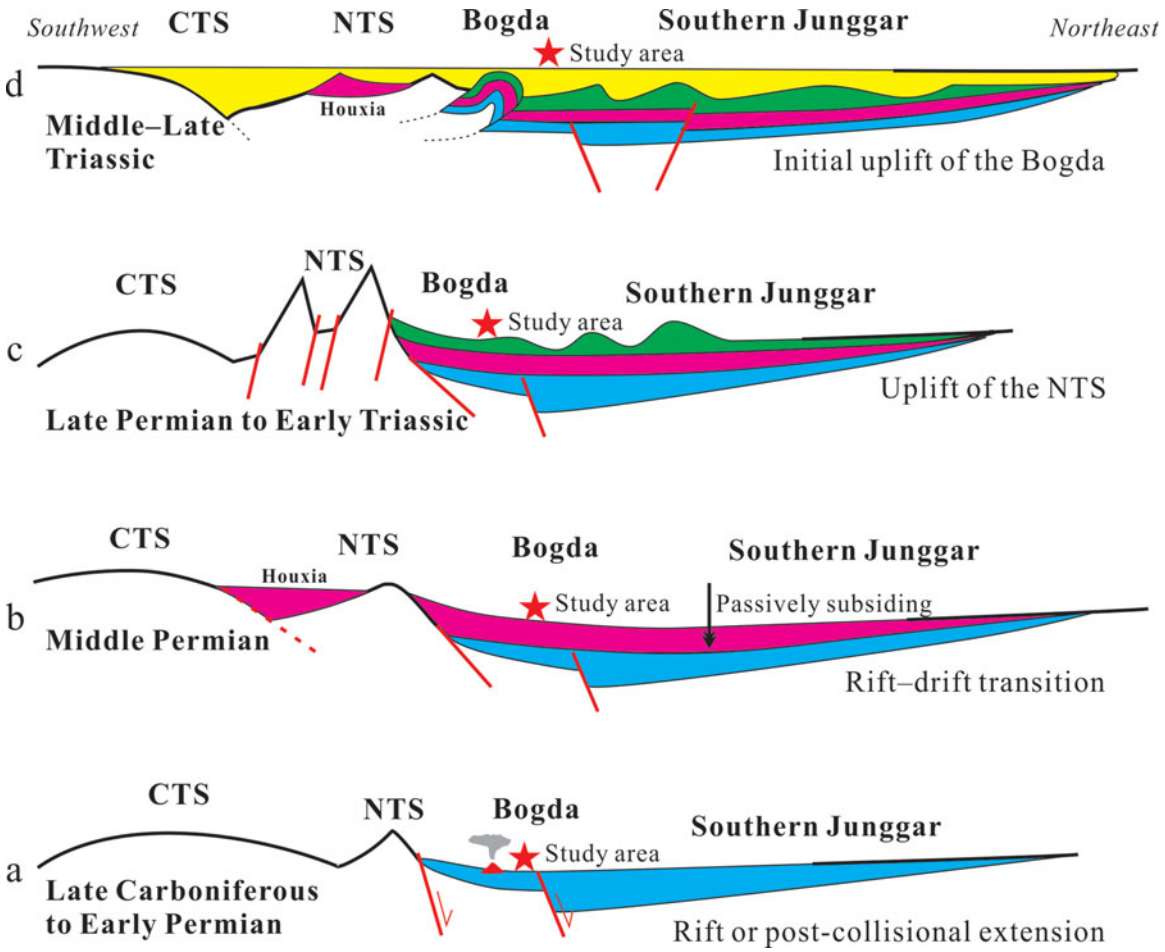

Figure 12. (Colour online) Reconstruction of key periods in the tectonic evolution of the Bogda Mountains/region from Late Carboniferous to Late Triassic time.

change (Wartes, Carroll & Greene, 2002). Therefore, we interpret this as passively subsiding during the rift-drift transition (Fig. 12b). This is consistent with the depositional unconformity between the Wulapo and Jingjingzigou formations investigated in the field section (Fig. 5b), which was possibly caused by the sudden fall of relative sea-level.

Afterwards, the Mid Permian Lower Lucaogou Formation (sample 12NFG-27), Upper Lucaogou Formation (sample 12NFG-30) and Hongyanchi Formation (15C-31) show some similarities with sample 15HXG-68 with one major NTS source. But the percentage of the older age group 360–320 Ma gradually increased (Fig. 9), implying the southern magmatic belt of the YCTS had joined the sources. The increased contribution from the southern margin of the YCTS implies the drainage system had widened again after the rift-drift transition.

6.c.3. Uplift of the NTS (Late Permian – Early Triassic)

The distribution of detrital zircon U–Pb ages in sample 15C-32 from the Upper Permian – Lower Triassic Cangfanggou Group shows a distinct Early Carboniferous peak age (328 Ma) and several Devonian ages. Combined with the NE-directed palaeocurrents, a single population peak and high quartz contents, this indicates a primary source of magmatic rocks in the southern margin of the YCTS. However, comparing this with the age spectra of the Mid Permian Hongyanchi Formation (sample 15C-31) and Mid Triassic Kelamayi Formation (sample 15C-2), those ages were expressed in sample 15C-31, but almost completely disappear in sample 15C-2. Furthermore, the slightly older peak age at 314 Ma in the Mid Triassic Kelamayi Formation (sample 15C-2) suggests the exhumation of an older and deeper source of the NTS. Thus, we attribute the provenance change to the uplift of the NTS in Late Permian – Early Triassic time (Fig. 12c). This interpretation is evidenced by the alluvial detritus which spread northeastwards in the NTS piedmont (Fig. 5c; Greene *et al*. 2001; Wang *et al*. 2016*b*) and the low-temperature thermochronology data in the region (Dumitru *et al*. 2001; Jolivet *et al*. 2010). Moreover, tectonic subsidence of the Southern Junggar Basin also accelerated during Late Permian time, creating accommodation for > 4000 m of non-marine sediments (Carroll *et al*. 1995; Wartes, Carroll & Greene, 2002), which accords with the uplift of the NTS. In addition, the missing Lower Triassic strata and the angular unconformity contact relationship between the Permian and Triassic rocks in the Aiweiergou area

https://doi.org/10.1017/S0016756816001217 Published online by Cambridge University Press

to the south also records the Late Permian – Early Triassic tectonic uplift of the NTS (Fig. 5d; Greene *et al*. 2001; Wartes, Carroll & Greene, 2002; Tang *et al*. 2014; Chen, Liao & Liu, 2015; Wang *et al*. 2016*b*).

It is also worth noting that the conformable contact relationship between the Triassic and Permian series in the Bogda suggests that the Late Permian – Early Triassic uplift was only limited to the NTS region to the south and did not affect the Bogda to the north (Tang *et al*. 2014). This is consistent with the same northward palaeocurrent direction on both sides of the Bogda, which indicates that the Bogda was not uplifted in Early Triassic time (Hendrix *et al*. 1992; Wartes, Carroll & Greene, 2002; Greene *et al*. 2005).

6.c.4. Initial uplift of the Bogda (Middle–Late Triassic)

Previous studies suggested that the Bogda had existed as a positive physiographic feature in Early Jurassic time based on the abrupt changes of sandstone composition and palaeocurrent direction in the southern Bogda (Hendrix *et al*. 1992; Greene *et al*. 2001, 2005), or the appearance of the Early Permian ages from the Lower Jurassic sample (Tang *et al*. 2014). However, our new data, coupled with recent studies, suggests the initial uplift of the Bogda occurred in Middle–Late Triassic time (Fig. 12d). The reasons are described as below: (1) The age spectrum of the Upper Triassic Haojiagou Formation (sample 15C-33) shows a significant multimodal distribution (Figs 8, 9). The multimodal spectrum implies the joining of other sources and a diversity of provenances in Late Triassic time. Moreover, this sample also presents a dramatic change with the first appearance of zircons from sub-contemporaneous Middle–Late Triassic magmatic sources (Fig. 8; peak ages of 243 and 234 Ma). Combined with the limited volume of the Triassic magmatism that occurred in the Bogda (BGMRXUAR, 1993; Wang *et al*. 2016*b*), we suggest the age group of 250–200 Ma in the detrital zircons probably came from the Bogda. (2) Sandstone compositional data reveals a sudden increase in Ls grains from the Mid–Upper Triassic samples. Moreover, the framework grain composition of these samples shows relative good sorting, abundant volcanic and quartz grains, and a mixed particle morphology (Fig. 5j), and displays the characteristics of sedimentary recycling on the Qt–F–L and Qm–F–Lt ternary diagrams (Fig. 6). These phenomena suggest the Bogda began to provide sedimentary materials. (3) The decrease in F grains from the Mid–Upper Triassic samples suggests less unroofing of the granitoids. Combined with the older and deeper Carboniferous rocks that had been erosionally unroofed in the NTS, the Early Permian detrital zircons (peak ages of 277 and 271 Ma) may have come from the NTS and the Bogda, which also proves the Bogda began to provide sources. (4) The depositional environments evolved from shallow-lacustrine systems to fluvial systems in Middle–Late Triassic time (Fig. 3), implying the Bogda had existed as a relatively positive topography. Upsection, the switching from NE- to N-directed palaeocurrents may maintain that the Bogda began to provide sources. (5) In the Dalongkou section, Jimusaer region, the Triassic series are overlain unconformably by the Lower Jurassic Badaowan Formation, revealing intensive tectonic activity in Late Triassic time (BGMRXUAR, 1999). In contrast, the five formations of the Upper Permian – Lower Triassic Cangfanggou Group are in conformable contact with each other, recording continuous sedimentation through the Permian–Triassic transition (Zhou *et al*. 1997; Metcalfe *et al*. 2009). The stratigraphic contact relationships propose that the initial uplift of the Bogda was not in Late Permian time, but most likely in Late Triassic time. And (6) the Triassic magmatism and ore-formation in the Eastern Tianshan were related to collisional crustal shortening and thickening (Gu *et al*. 2006; Deng *et al*. 2017), revealing an Indosinian (Triassic) orogenic event (Gu *et al*. 2006). All the evidence suggests that the Bogda was a gentle positive relief providing sedimentary materials to the Junggar Basin in Middle–Late Triassic time. In addition, it is important to note that the sample 15GG-01 from the Xiaoquangou Group lacks precise dating ages or biostratigraphy, which cannot constrain its accurate age. Thus, we mark the initial uplift and erosion of the palaeo-Bogda as occurring in Middle–Late Triassic time, and most likely in Late Triassic time.

Combining this with the Early Carboniferous ages (peak at 336 Ma), Late Carboniferous ages (peak at 303 Ma) and Permian ages (peaks at 293 Ma and 271 Ma) that exist in the spectrograms of the detrital zircons, we suggest the provenance of the Middle–Late Triassic samples mainly include the Bogda, NTS and YCTS. Furthermore, considering the YCTS also became the source area of the basin, together with the extensive lacustrine deposits in the Junggar Basin and its adjacent regions (Li & Peng, 2013), we suggest the further expansion of the basin drainage system during Middle–Late Triassic time, as well as Early–Middle Jurassic time (Yang *et al*. 2012*a*; Tang *et al*. 2014). This is consistent with the southern edge of the Junggar Basin extending at least into the Houxia area during Middle–Late Triassic time, where the Mid–Upper Triassic Xiaoquangou Group overlies unconformably the Mid Permian Lucaogou Formation (Fig. 5d; Wartes, Carroll & Greene, 2002; Chen, Liao & Liu, 2015; Wang *et al*. 2016*b*). Numerous studies indicated that the Tianshan and its adjacent regions were a peneplain during Early Jurassic time, and the Tianshan had a relatively gentle palaeogeomorphology (e.g. Li & Peng, 2013; Tang *et al*. 2014). Thus, the expanded drainage system, the relatively low topography and the weakened uplift of the Tianshan also suggest a levelled process from Middle–Late Triassic to Early–Middle Jurassic times (Tang *et al*. 2014).

https://doi.org/10.1017/S0016756816001217 Published online by Cambridge University Press

7. Conclusions

The integrated provenance techniques employed here for the Bogda revealed a series of shifts in the geochronology, palaeocurrents and sandstone composition from Late Carboniferous to Late Triassic time. These analyses, combined with the published data, led us to draw the following conclusions:

(1) The U–Pb detrital zircon ages range widely from 2421 to 213 Ma and can be divided into six groups: 2421–541 Ma, 541–360 Ma, 360–320 Ma, 320–300 Ma, 300–250 Ma and 250–200 Ma. Those groups, together with the available palaeocurrent measurements, indicate that the 2421–541 Ma, 541–360 Ma and 360–320 Ma age groups were assigned to the Precambrian basement and magmatic rocks of the YCTS, and the 320–300 Ma age group was related to the volcanic island arc in the NTS and northern margin of the YCTS. Furthermore, the 250–200 Ma age group corresponded to the Middle–Late Triassic volcanism in the Bogda. (2) The initial tectonic setting of the Bogda in Carboniferous–Early Permian time was an extensional context, which was related to rifting or post-collision. (3) The tectonic evolution of the Bogda can be divided into four stages: rift or post-collisional extension from Late Carboniferous to Early Permian time, rift-drift transition in Middle Permian time, uplift of the NTS during Late Permian – Early Triassic time, and the initial uplift of the Bogda in Middle–Late Triassic time.

Acknowledgements. We thank Editor-in-Chief Prof. Mark Allen and two anonymous reviewers for their constructive comments and careful corrections that led to significant improvement of the manuscript. We express our gratitude to Dr Rong Chen, Dr Jian Ma and Dr Yizhe Wang for their discussion and field assistance. This work was financially supported by the National Science and Technology Major Project of China (Grant No. 2011ZX05009–001).

Supplementary material

To view supplementary material for this article, please visit https://doi.org/10.1017/S0016756816001217.

References

Allen, M. B., Şengör, A. M. C. & Natal'in, B. A. 1995. Junggar, Turpan, and Alakol basins as Late Permian to ?Early Triassic extensional structures in a sinistral shear zone in the Altaid orogenic collage, central Asia. *Journal of the Geological Society, London* **152**, 327–38.

Allen, M. B., Windley, B. F. & Zhang, C. 1993. Paleozoic collisional tectonics and magmatism of the Chinese Tian Shan, central Asia. *Tectonophysics* **220**, 89–115.

Andersen, T. 2002. Correction of common lead in U–Pb analyses that do not report ^{204}Pb. *Chemical Geology* **192**, 59–79.

Andersen, T. 2005. Detrital zircons as tracers of sedimentary provenance: limiting conditions from statistics and numerical simulation. *Chemical Geology* **216**, 249–70.

Bgmrxuar (Bureau Of Geology And Mineral Resources Of Xinjiang Uygur Autonomous Region). 1993. *Regional Geology of Xinjiang Uygur Autonomous Region*. Beijing: Geological Publishing House (in Chinese).

Bgmrxuar (Bureau of Geology and Mineral Resources of Xinjiang Uygur Autonomous Region). 1999. *Lithostratigraphy of Xinjiang Uygur Autonomous Region*. Wuhan: China University of Geosciences Press (in Chinese).

Cai, Z. X., Chen, F. J. & Jia, Z. Y. 2000. Types and tectonic evolution of Junggar Basin. *Earth Science Frontiers* **7**, 431–40 (in Chinese with English abstract).

Carroll, A. R., Graham, S. A., Hendrix, M. S., Ying, D. & Zhou, D. 1995. Late Paleozoic tectonic amalgamation of northwestern China: sedimentary record of the northern Tarim, northwestern Turpan, and southern Junggar Basins. *Geological Society of America Bulletin* **107**, 571–94.

Carroll, A. R., Graham, S. A. & Smith, M. E. 2010. Walled sedimentary basins of China. In *Tectonic and Stratigraphic Evolution of Nonmarine Basins of China* (eds S. A. Graham, A. R. Carroll & L Ping). *Basin Research* **22**, 7–32.

Charvet, J., Shu, L. S. & Laurent-Charvet, S. 2007. Paleozoic structural and geodynamic evolution of eastern Tianshan (NW China): welding of the Tarim and Junggar plates. *Episodes* **30**, 162–86.

Charvet, J., Shu, L. S., Laurent-Charvet, S., Wang, B., Michel, F., Dominique, C., Chen, Y. & Koen, D. J. 2011. Paleozoic tectonic evolution of the Tianshan belt, NW China. *Science China Earth Sciences* **54**, 166–84.

Chen, Z. Q., Liao, Z. T. & Liu, L. J. 2015. Correction of two Upper Paleozoic stratigraphic units in the Tianshan Mountains region, Xinjiang Uygur Autonomous Region and implications on the Late Paleozoic evolution of Tianshan tectonic complex, Northwest China. *Journal of Palaeogeography* **4**, 358–70.

Chen, X. J., Shu, L. S. & Santosh, M. 2011. Late Paleozoic post-collisional magmatism in the Eastern Tianshan Belt, Northwest China: new insights from geochemistry, geochronology and petrology of bimodal volcanic rocks. *Lithos* **127**, 581–98.

Chen, X. J., Shu, L. S., Santosh, M. & Zhao, X. X. 2013. Island arc-type bimodal magmatism in the eastern Tianshan Belt, Northwest China: geochemistry, zircon U–Pb geochronology and implications for the Paleozoic crustal evolution in Central Asia. *Lithos* **168–69**, 48–66.

Chen, F. J., Wang, X. W. & Wang, X. W. 2005. Prototype tectonic evolution of Junggar Basin, Northwestern China. *Earth Science Frontiers* **12**, 77–89 (in Chinese with English abstract).

Chen, Y. B., Zhang, G. W., Liu, X. M., Xiong, X. L., Yuan, C. & Chen, L. L. 2012. Zircons LA-ICP-MS U–Pb dating on the Baluntai deformed granitoids, Central Tianshan Block, Northwest China and its tectonic implications. *Geological Review* **58**, 117–25 (in Chinese with English abstract).

Chen, S. P., Zhang, Y. W., Tang, L. J. & Bai, G. P. 2001. Tectonic evolution of the Junggar Basin in the Late Carboniferous–Permian. *Acta Geological Sinica* **75**, 398–408 (in Chinese with English abstract).

Chen, J. F., Zhou, T. X., Xie, Z., Zhang, X. & Guo, X. S. 2000. Formation of positive $\varepsilon_{Nd}(T)$ granitoids from the Alataw Mountains, Xinjiang, China, by mixing and fractional crystallization: implication for Phanerozoic crustal growth. *Tectonophysics* **328**, 53–67.

Chen, Z. Q. & Shi, G. R. 2003. Late Paleozoic depositional history of the Tarim basin, northwest China: an integration of biostratigraphic and lithostratigraphic

constraints. *American Association of Petroleum Geologists Bulletin* **87**, 1323–135.

Corfu, F., Hanchar, J. M., Hoskin, P. W. O. & Kinny, P. 2003. Atlas of zircon textures. *Zircon: Reviews in Mineralogy and Geochemistry* **53**, 469–500.

Deng, X. H., Chen, Y. J., Santosh, M., Wang, J. B., Li, C., Yue, S. W., Zheng, Z., Chen, H. J., Tang, H. S., Dong, L. H. & Qu, X. 2017. U–Pb zircon, Re–Os molybdenite geochronology and Rb–Sr geochemistry from the Xiaobaishitou W (–Mo) deposit: implications for Triassic tectonic setting in eastern Tianshan, NW China. *Ore Geology Reviews* **80**, 332–51.

Dickinson, W. R. 1985. Interpreting provenance relations from detrital modes of sandstones. *Provenance of Arenites* (ed. G. G. Zuffa), pp. 333–61.

Dickinson, W. R., Beard, L. S., Brackenbridge, G. R., Erjavec, J. L., Ferguson, R. C., Inman, K. F., Knepp, R. A., Lindberg, F. A. & Ryberg, P. T. 1983. Provenance of North-American Phanerozoic sandstones in relation to tectonic setting. *Geological Society of America Bulletin* **94**, 222–35.

Dumitru, T. A., Zhou, D., Chang, E. Z. & Graham, S. A. 2001. Uplift, exhumation, and deformation in the Chinese Tian Shan, in Paleozoic and Mesozoic tectonic evolution of central Asia: from continental assembly to intracontinental deformation. *Geological Society of America Memoir* **194**, 71–99.

Fang, S. H., Jia, C. Z., Guo, Z. J., Song, Y., Xu, H. M. & Liu, L. J. 2006. New view on the Permian evolution of the Junggar Basin and its implications for tectonic evolution. *Earth Science Frontiers* **13**, 108–21 (in Chinese with English abstract).

Fang, S. H., Song, Y., Jia, C. Z., Wang, X. L. & Yuan, Q. D. 2007. The Mesozoic–Cenozoic clastic composition of Bogda area, Xinjiang: implications on the evolution of basin–range pattern. *Acta Geological Sinica* **81**, 1229–36 (in Chinese with English abstract).

Gao, J., He, G. Q., Li, M. S., Xiao, X. C., Tang, Y. Q., Wang, J. & Zhao, M. 1995. The mineralogy, petrology, metamorphic PTDt trajectory and exhumation mechanism of blueschists, South Tianshan, northwestern China. *Tectonophysics* **250**, 151–68.

Gao, J., Klemd, R., Qian, Q., Zhang, X., Li, J. L., Jiang, T. & Yang, Y. Q. 2011. The collision between the Yili and Tarim blocks of the Southwestern Altaids: geochemical and age constraints of a leucogranite dike crosscutting the HP–LT metamorphic belt in the Chinese Tianshan Orogen. *Tectonophysics* **499**, 118–31.

Gao, J. G., Li, W. Y., Guo, X. C., Zhou, Y., Liu, J. C., Fang, T. B. & Zhou, R. H. 2013. Studies on the geochemistry, zircon U–Pb age and geological significance of diabase in the Sepikou region, eastern Bogda, Xinjiang. *Xinjiang Geology* **31**, 117–23 (in Chinese with English abstract).

Gao, J. G., Li, W. Y., Liu, J. C., Gao, Y. X., Guo, X. C., Zhou, Y. & Fang, T. B. 2014. Geochemistry, zircon U–Pb age and Hf isotopes of Late Carboniferous rift volcanic in the Sepikou region, eastern Bogda, Xinjiang. *Acta Petrologica Sinica* **30**, 3539–52 (in Chinese with English abstract).

Gao, J., Li, M. S., Xiao, X. C., Tang, Y. Q. & He, G. Q. 1998. Paleozoic tectonic evolution of the Tianshan orogen, northwestern China. *Tectonophysics* **287**, 213–31.

Gao, J., Long, L. L., Klemd, R., Qian, Q., Liu, D. Y., Xiong, X. M., Su, W., Liu, W., Wang, Y. T. & Yang, F. Q. 2009. Tectonic evolution of the South Tianshan orogen and adjacent regions, NW China: geochemical and age constraints of granitoid rocks. *International Journal of Earth Sciences* **98**, 1221–38.

Gehrels, G. 2014. Detrital zircon U–Pb geochronology applied to tectonics. *Annual Review of Earth and Planetary Sciences* **42**, 127–49.

Gehrels, G. E., Yin, A. & Wang, X. F. 2003. Detrital-zircon geochronology of the northeastern Tibetan plateau. *Geological Society of America Bulletin* **115**, 881–96.

Greene, T. J., Carroll, A. R., Hendrix, M. S., Graham, S. A., Wartes, M. A. & Abbink, O. A. 2001. Sedimentary record of Mesozoic deformation and inception of the Turpan–Hami basin, northwest China. *Geological Society of America Memoir* **194**, 317–40.

Greene, T. J., Carroll, A. R., Wartes, M., Graham, S. A. & Wooden, J. L. 2005. Integrated provenance analysis of a complex orogenic terrane: Mesozoic uplift of the Bogda Shan and inception of the Turpan–Hami Basin, NW China. *Journal of Sedimentary Research* **75**, 251–67.

Gu, L. X., Hu, S. X., Yu, C. S., Zhao, M., Wu, C. Z. & Li, H. Y. 2001. Intrusive activities during compression-extension tectonic conversion in the Bogda intracontinental orogen. *Acta Petrologica Sinica* **17**, 187–98 (in Chinese with English abstract).

Gu, L. X., Yu, C. S., Hu, S. X. & Li, H. Y. 2000. Carboniferous vulcanites in the Bogda orogenic belt of eastern Tianshan: their tectonic implications. *Acta Petrologica Sinica* **16**, 305–16 (in Chinese with English abstract).

Gu, L. X., Zhang, Z. Z., Wu, C. Z., Tang, J. H., Wang, C. S., Xi, A. H. & Zheng, Y. C. 2006. Some problems on granites and vertical growth of the continental crust in the eastern Tianshan, NW China. *Acta Petrologica Sinica* **22**, 1103–20 (in Chinese with English abstract).

Guo, W., Zhou, D. W., Ouyang, Z. J. & Zhou, X. H. 2009. Formation and its geological environment of the Permian magmatic rocks in Donggou county, Daban city, southern margin of Bogda orogenic belt. *Journal of Shanxi Normal University (Natural Science Edition)* **37**, 103–08 (in Chinese with English abstract).

Han, B. F., Guo, Z. J., Zhang, Z. C., Zhang, L., Chen, J. F. & Song, B. 2010. Age, geochemistry, and tectonic implications of a late Paleozoic stitching pluton in the North Tian Shan suture zone, western China. *Geological Society of American Bulletin* **122**, 627–40.

Han, B. F., He, G. Q., Wang, X. C. & Guo, Z. J. 2011. Late Carboniferous collision between the Tarim and Kazakhstan–Yili terranes in the western segment of the South Tian Shan Orogen, Central Asia, and implications for the Northern Xinjiang, western China. *Earth-Science Reviews* **109**, 74–93.

Han, B. F., He, G. Q., Wu, T. R. & Li, H. M. 2004. Zircon U–Pb dating and geochemical features of Early Paleozoic granites from Tianshan, Xinjiang: implications for tectonic evolution. *Xinjiang Geology* **22**, 4–11 (in Chinese with English abstract).

He, G. Q., Li, M. S., Liu, D. Q. & Zhou, R. H. 1994. *Paleozoic Crustal Evolution and Mineralization in Xinjiang of China*. Xinjiang: Xinjiang People's Publishing House, 437 pp (in Chinese with English abstract).

Hendrix, M. S. 2000. Evolution of Mesozoic sandstone compositions, southern Junggar, northern Tarim, and western Turpan basins, Northwest China: a detrital record of the ancestral Tian Shan. *Journal of Sedimentary Research* **70**, 520–32.

Hendrix, M. S., Graham, S. A., Carroll, A. R., Sobel, E. R., Mcknight, C. L., Schulein, B. J. & Wang, Z. X. 1992. Sedimentary record and climatic

https://doi.org/10.1017/S0016756816001217 Published online by Cambridge University Press

implications of recurrent deformation in the Tian Shan: evidence from Mesozoic strata of the North Tarim, South Junggar and Turpan basins, Northwest China. *Geological Society of America Bulletin* **104**, 53–79.

Hu, A., Jahn, B. M., Zhang, G., Chen, Y. & Zhang, Q. 2000. Crustal evolution and Phanerozoic crustal growth in northern Xinjiang: Nd isotopic evidence. Part I. Isotopic characterization of basement rocks. *Tectonophysics* **328**, 15–51.

Ingersoll, R. V., Bulard, T. F., Ford, R. L., Grimn, J. P., Pickle, J. P. & Sares, S. W. 1984. The effect of grain-size on detrital modes—a test of the Gazzi–Dickinson point-counting method. *Journal of Sedimentary Petrology* **54**, 103–16.

Jackson, S. E., Pearson, N. J., Griffin, W. L. & Belousova, E. A. 2004. The application of laser ablation-inductively coupled plasma-mass spectrometry to in situ U–Pb zircon geochronology. *Chemical Geology* **211**, 47–69.

Jahn, B. M., Wu, F. Y. & Chen, B, B. 2000. Granitoids of the Central Asian orogenic belt and continental growth in the Phanerozoic. *Transactions of the Royal Society of Edinburgh: Earth Sciences* **91**, 181–93.

Jolivet, M., Dominguez, S., Charreau, J., Chen, Y., Li, Y. A. & Wang, Q. C. 2010. Mesozoic and Cenozoic tectonic history of the Central Chinese Tian Shan: reactivated tectonic structures and active deformation. *Tectonics* **29**, TC6019. doi: 10.1029/2010TC002712.

Laurent-Charvet, S., Monié, P., Charvet, J., Shu, L. S. & Ma, R. S. 2003. Late Paleozoic strike-slip shear zones in northeastern Xinjiang (NW China): new structural and geochronological data. *Tectonics* **22**, 1099–101.

Lawton, T. F. & Trexler, J. H. 1991. Piggyback basin in the Sevier orogenic belt, Utah: implications for development of the thrust wedge: *Geology* **19**, 827–30.

Li, Z. & Chen, B. 2014. Geochronology and geochemistry of the Paleoproterozoic meta-basalts from the Jiao-Liao-Ji Belt, North China Craton: implications for petrogenesis and tectonic setting. *Precambrian Research* **255**, 653–67.

Li, Z., Chen, B. & Wei, C. J. 2016. Is the Paleoproterozoic Jiao-Liao-Ji Belt (North China Craton) a rift? *International Journal of Earth Sciences*, published online 12 April 2016. doi: 10.1007/s00531-016-1323-2.

Li, Z., Chen, B., Wei, C. J., Wang, C. X. & Han, W. 2015. Provenance and tectonic setting of the Paleoproterozoic metasedimentary rocks from the Liaohe Group, Jiao-Liao-Ji Belt, North China Craton: insights from detrital zircon U–Pb geochronology, whole-rock Sm–Nd isotopes, and geochemistry. *Journal of Asian Earth Sciences* **111**, 711–32.

Li, P., Liu, W., Zhu, Z. X., Chen, C., Chen, B. X. & Jin, L. Y. 2013*a*. SHRIMP zircon U–Pb age of quartz monzonite in the west of Bogda Mountain, Xinjiang, China, and its geological significance. *Journal of Xinjiang University (Natural Science Edition)* **30**, 476–81 (in Chinese with English abstract).

Li, P., Liu, W., Zhu, Z. X., Chen, C., Jin, L. Y., Xu, S. Q., Zhao, T. Y. & Chen, B. X. 2013*b*. Geochemical characteristics, geochronology and its geological significance of quartz diorite in Sangeshan Area, west of Bogda, Xinjiang. *Xinjiang Geology* **31**, 162–66 (in Chinese with English abstract).

Li, Z. & Peng, S. T. 2013. U–Pb geochronological records and provenance system analysis of the Mesozoic–Cenozoic sandstone detrital zircons in the northern and southern piedmonts of Tianshan, Northwest China: responses to intracontinental basin-range evolution. *Acta Petrologica Sinica* **29**, 739–55 (in Chinese with English abstract).

Li, Z., Tang, W. X., Peng, S. T. & Xu, J. Q. 2012. Detrital zircon U–Pb geochronological and depositional records of the Mesozoic–Cenozoic profile in the southern Junggar Basin, northwest China, and their responses to basin-range tectonic evolution. *Chinese Journal of Geology* **47**, 1016–40 (in Chinese with English abstract).

Li, C., Xiao, W. J., Han, C. M., Zhou, K. F. & Zhang, Z. X. 2013*c*. SIMS zircon U–Pb age of the plagiogranites from Kuitun River ophiolite and its tectonic implications. *Chinese Journal of Geology* **48**, 815–26 (in Chinese with English abstract).

Liang, T., Guo, X. C., Gao, J. G., Fan, T. B., Qin, H. F., Zhou, R. H. & Hei, H. 2011. Geochemistry and structure characteristic of Carboniferous volcanic rocks in the eastern of Bogeda Mountain. *Xinjiang Geology* **29**, 289–95 (in Chinese with English abstract).

Liu, D. D., Guo, Z. J. & Zhang, Z. Y. 2013. A new viewpoint of the Aiweiergou unconformity, Northern Tian Shan, Xinjiang. *Geotectonica et Metallogenia* **37**, 349–65 (in Chinese with English abstract).

Liu, D. D., Guo, Z. J., Zhang, Z. C. & Wu, C. D. 2012. The Late Paleozoic tectonic relationship between the Tian Shan orogenic belt and Junggar basin: constraints from zircon SHRIMP U–Pb dating and geochemistry characteristics of volcanic rocks in Arbasay Formation. *Acta Petrologica Sinica* **28**, 2355–68 (in Chinese with English abstract).

Liu, Z. Q., Han, B. F., Ji, J. Q. & Li, Z. H. 2005. Ages and geochemistry of the post-collisional granitic rocks from Eastern Alataw Mountains, Xinjiang, and implications for vertical growth. *Acta Petrologica Sinica* **21**, 623–39 (in Chinese with English abstract).

Liu, F., Yang, J. S., Li, T. F., Chen, S. Y., Xu, X. Z., Li, J. Y. & Jia, Y. 2011. Geochemical characteristics of Late Carboniferous volcanic rocks in northern Tianshan, Xinjiang, and their geological significance. *Geology in China* **38**, 858–89 (in Chinese with English abstract).

Long, L. L., Gao, J., Klemd, R., Beier, C., Qian, Q., Zhang, X., Wang, J. B. & Jiang, T. 2011. Geochemical and geochronological studies of granitoid rocks from the Western Tianshan Orogen: implications for continental growth in the southwestern Central Asian Orogenic Belt. *Lithos* **126**, 321–40.

Ludwig, K. R. 2003. *ISOPLOT 3: A Geochronological Toolkit for Microsoft Excel*. Berkeley Geochronology Centre, Special Publication 4, 1–74.

Ma, R. S., Shu, L. S. & Sun, J. Q. 1997. *Tectonic Evolution and Metallization in the Eastern Tianshan Belt, China*. Beijing: Geological Publishing House, 202 pp. (in Chinese with English abstract).

Metcalfe, I., Foster, C. B., Afonin, S. A., Nicoll, R. S., Mundil, R., Wang, X. F. & Lucas, S. G. 2009. Stratigraphy, biostratigraphy and C-isotopes of the Permian–Triassic nonmarine sequence at Dalongkou and Lucaogou, Xinjiang Province, China. *Journal of Asian Earth Sciences* **36**, 503–20.

Nie, J. S., Horton, B. K., Saylor, J. E., Mora, A., Mange, M., Garzione, C. N., Basu, A., Moreno, C. J., Caballero, V. & Parra, M. 2012. Integrated provenance analysis of a convergent retroarc foreland system: U–Pb ages, heavy minerals, Nd isotopes, and sandstone compositions of the Middle Magdalena Valley basin, northern Andes, Colombia. *Earth-Science Reviews* **110**, 111–26.

Ouyang, Z. J., Zhou, D. W., Lin, J. Y. & Feng, J. P. 2006. Geochemistry and geological implications of the Baiyanghe basic–intermediate dyke swarm in the Bogda orogenic belt in Xinjiang, China. *Geotectonica et Metallogenia* **30**, 495–503 (in Chinese with English abstract).

Pearce, J. A. 1996. Sources and settings of granitic rocks. *Episodes* **19**, 120–5.

Pearce, J. A. 2008. Geochemical fingerprinting of oceanic basalts with applications to ophiolite classification and the search for Archean oceanic crust. *Lithos* **100**, 14–48.

Peccerillo, A. & Taylor, A.R. 1976. Geochemistry of Eocene calc-alkaline volcanic rocks from the Kastamonu area, Northern Turkey. *Contributions to Mineralogy and Petrology* **58**, 63–81.

Pupin, J. P. 1980. Zircon and granite petrology. *Contributions to Mineralogy and Petrology* **73**, 207–20.

Qiu, N. S., Zhang, Z. H. & Xu, E. S. 2008. Geothermal regime and Jurassic source rock maturity of the Junggar Basin, northwest China. *Journal of Asian Earth Sciences* **31**, 4–6.

Şengör, A. C., Natal'in, B. A. & Burtman, V. S. 1993. Evolution of the Altaid tectonic collage and Palaeozoic crustal growth in Eurasia. *Nature* **364**, 299–307.

Shu, L. S., Wang, B., Zhu, W. B., Guo, Z. J., Charvet, J. & Zhang, Y. 2011. Timing of initiation of extension in the Tianshan, based on structural, geochemical and geochronological analyses of bimodal volcanism and olistostrome in the Bogda Shan (NW China). *International Journal of Earth Sciences* **100**, 1647–63.

Shu, L. S., Zhu, W. B., Wang, B., Faure, M., Charvet, J. & Cluzel, D. 2005. The post-collision intracontinental rifting and olistostrome on the southern slope of Bogda Mountains, Xinjiang. *Acta Petrologica Sinica* **21**, 25–36 (in Chinese with English abstract).

Si, G. H., Su, H. P., Yang, G. H., Zhang, C. & Yang, G. X. 2014. Geological significance and geochemical characteristics of the Sikeshu pluton in North Tianshan, Xinjiang. *Xinjiang Geology* **32**, 19–24 (in Chinese with English abstract).

Tang, G. J., Wang, Q., Wyman, D. A., Sun, M., Li, Z. X., Zhao, Z. H., Sun, W. D., Jia, X. H. & Jiang, Z. Q. 2010. Geochronology and geochemistry of Late Paleozoic magmatic rocks in the Lamasu–Dabate area, northwestern Tianshan (west China): evidence for a tectonic transition from arc to post-collisional setting. *Lithos* **119**, 393–411.

Tang, G. J., Wang, Q., Zhao, Z. H., Wyman, D. A., Jiang, Z. Q. & Jia, X. H. 2008. Geochronological age and tectonic background of the Dabate A-type pluton in the west Tianshan. *Acta Petrologica Sinica* **24**, 947–58 (in Chinese with English abstract).

Tang, W. H., Zhang, Z. C., Li, J. F., Li, K., Chen, Y. & Guo, Z. J. 2014. Late Paleozoic to Jurassic tectonic evolution of the Bogda area (northwest China): evidence from detrital zircon U–Pb geochronology. *Tectonophysics* **626**, 144–56.

Wang, F. C. & Cai, X. J. 2010. Geochemical characteristics and tectonic significance of the Late Paleozoic granites in eastern Bogda Mountains, Xinjiang. *Journal of Lanzhou University (Natural Sciences)* **46**, 1–6 (in Chinese with English abstract).

Wang, X. W., Cui, F. L., Sun, J. M., Zhu, X. H., Zhu, T. & Bai, J. K. 2015*a*. Geochemical characteristics, geochronology and its geological significance of the diorite in Shagoukuduke area, east of the Bogda Orogenic Belt. *Xinjiang Geology* **33**, 151–8 (in Chinese with English abstract).

Wang, X. W., Cui, F. L., Sun, J. M., Zhu, X. H., Bai, J. K. & Zhu, T. 2015*b*. Geochemical characteristics and its significance of the Early Carboniferous bimodal volcanic rocks in Jijitazi area, east of the Bogda Orogenic Belt. *Northwestern Geology* **48**, 100–14 (in Chinese with English abstract).

Wang, B., Faure, M., Cluzel, D., Shu, L. S., Charvet, J., Meffre, S. & Ma, Q. 2006. Late Paleozoic tectonic evolution of the northern west Chinese Tianshan Belt. *Geodinamica Acta* **19**, 237–47.

Wang, B., Faure, M., Shu, L. S., Jong, K., Charvet, J., Cluzel, D., Jahn, B. M., Chen, Y. & Ruffet, G. 2010*a*. Structural and geochronological study of high-pressure metamorphic rocks in the Kekesu Section (Northwestern China): implications for the Late Paleozoic tectonics of the Southern Tianshan. *Journal of Geology* **118**, 59–77.

Wang, J. R., Li, D. T., Tian, L. P., Yu, M., Wang, H. T., Zhao, Z. X. & Tang, Z. L. 2010*b*. Late Paleozoic tectono-magmatic evolution in Bogda Orogenic Belt, Xinjiang: evidence from geochemistry of volcanic rocks. *Acta Petrologica Sinica* **26**, 1103–15 (in Chinese with English abstract).

Wang, Z. X., Li, T., Zhou, G. Z., Lu, M. A., Liu, Y. Q. & Li, Y. 2003. Geological record of the Late Carboniferous orogeny in Bogdashan, Northern Tianshan Mountains, Northwest China. *Earth Science Frontiers* **10**, 63–9 (in Chinese with English abstract).

Wang, B., Shu, L. S., Cluzel, D., Faure, M. & Charvet, J. 2007a. Geochemical constraints on Carboniferous volcanic rocks of the Yili Block (Xinjiang, NW China): implication for the tectonic evolution of western Tianshan. *Journal of Asian Earth Sciences* **29**, 148–59.

Wang, B., Shu, L. S., Cluzel, D., Faure, M. & Charvet, J. 2007b. Geochronological and geochemical studies on the Boruhoro plutons, north of Yili, NW Tianshan and their tectonic implication. *Acta Petrologica Sinica* **23**, 1885–900 (in Chinese with English abstract).

Wang, B., Shu, L. S., Faure, M., Cluzel, D. & Charvet, J. 2007*c*. Paleozoic tectonism and magmatism of Kekesu-Qiongkushitai section in southwestern Chinese Tianshan and their constraints on the age of the orogeny. *Acta Petrologica Sinica* **23**, 1354–68 (in Chinese with English abstract).

Wang, B., Shu, L. S., Faure, M., Jahn, B. M., Cluzel, D., Charvet, J., Chung, S. L. & Meffre, S. 2011. Paleozoic tectonics of the southern Tianshan: new insights from structural, chronological and geochemical studies of the Heiyingshan ophiolitic mélange (NW China). *Tectonophysics* **497**, 85–104.

Wang, J. L., Wang, S. J. & Liu, X. M. 2009. Geochemistry, geochronology and geological significance of alkali-feldspar granite from Tianger area, Xinjiang. *Acta Petrologica Sinica* **25**, 925–33 (in Chinese with English abstract).

Wang, J. L., Wu, C. D., Li, Z., Zhu, W., Chen, Y. W., Li, Q. Y., Wu, J., Deng, L. J. & Chen, R. 2016*a*. Geochronology and geochemistry of volcanic rocks in the Arbasay Formation, Xinjiang Province (Northwest China): implications for the tectonic evolution of the North Tianshan. *International Geology Review*, published online 31 May 2016. doi: 10.1080/00206814.2016.1185750.

Wang, J. L., Wu, C. D., Zhu, W., Li, Z., Wu, J., Chen, R. & Wang, J. 2016*b*. Tectonic-depositional environment and prototype basin evolution of the Permian–Triassic

in the southern Junggar Basin. *Journal of Palaeogeography* **18**, 643–60 (in Chinese with English abstract).

Wang, Q., Wyman, D. A., Zhao, Z. H., Xu, J. F., Bai, Z. H., Xiong, X. L., Dai, T. M., Li, C. F. & Chu, Z. Y. 2007*d*. Petrogenesis of Carboniferous adakites and Nb-enriched arc basalts in the Alataw area, northern Tianshan Range (western China): implications for Phanerozoic crustal growth in the Central Asia orogenic belt. *Chemical Geology* **236**, 42–64.

Wang, X. W., Xu, X. Y., Ma, Z. P., Chen, J. L., Cui, F. L., Zhu, X. H. & Sun, J. M. 2015*c*. Geochemistry and tectonic setting of the early Carboniferous volcanic rocks in the eastern section of the Bogda orogenic belt in Xinjiang. *Geology and Exploration* **51**, 108–22 (in Chinese with English abstract).

Wang, X. W., Xu, X. Y., Ma, Z. P., Chen, J. L., Zhu, X. H., Sun, J. M. & Cui, F. L. 2015*d*. Geochemical characteristics and its geological significance of the Early Carboniferous bimodal volcanic rocks in Saerqiaoke area, east of the Bogda Orogenic Belt. *Geological Science and Technology Information* **34**, 58–70 (in Chinese with English abstract).

Wang, X. W., Xu, X. Y., Ma, Z. P., Chen, J. L., Zhu, X. H., Sun, J. M. & Cui, F. L. 2015*e*. Geochemical characteristics of the Late Carboniferous bimodal volcanic rocks in Jijitaizi area, eastern Bogda orogenic belt, and their geological significance. *Geology in China* **42**, 553–69 (in Chinese with English abstract).

Wartes, M. A., Carroll, A. R. & Greene, T. J. 2002. Permian sedimentary record of the Turpan-Hami basin and adjacent regions, northwest China: constraints on postamalgamation tectonic evolution. *Geological Society of America Bulletin* **114**, 131–52.

Windley, B. F., Alexeiev, D., Xiao, W. J., Kröner, A. & Badarch, G. 2007. Tectonic models for accretion of the Central Asian Orogenic Belt. *Journal of the Geological Society, London* **164**, 31–47.

Wong, K., Sun, M., Zhao, G. C., Yuan, C. & Xiao, W. J. 2010. Geochemical and geochronological studies of the Alegedayi Ophiolitic Complex and its implication for the evolution of the Chinese Altai. *Gondwana Research* **18**, 438–54.

Wood, D. A. 1980. The application of a Th-Hf-Ta diagram to problems of tectonomagmatic classification and to establishing the nature of crustal contamination of basaltic lavas of the British Tertiary volcanic province. *Earth and Planetary Science Letters* **50**, 11–30.

Xia, L. Q., Xia, Z. C., Xu, X. Y., Li, X. F., Ma, Z. P. & Wang, L. S. 2004*a*. Carboniferous Tianshan igneous mega province and mantle plume. *Geological Bulletin of China* **23**, 903–10 (in Chinese with English abstract).

Xia, L. Q., Xu, X. Y., Xia, Z. C., Li, X. M., Ma, Z. P. & Wang, L. S. 2004*b*. Petrogenesis of Carboniferous rift-related volcanic rocks in the Tianshan, northwestern China. *Geological Society of America Bulletin* **116**, 419–33.

Xiao, W. J., Windley, B. F., Huang, B. C., Han, C. M., Yuan, C., Chen, H. L., Sun, M., Sun, S. & Li, J. L. 2009. End-Permian to mid-Triassic termination of the accretionary processes of the southern Altaids: implications for the geodynamic evolution, Phanerozoic continental growth, and metallogeny of Central Asia. *International Journal of Earth Sciences* **98**, 1189–217.

Xie, W., Luo, Z. Y., Xu, Y. G., Chen, Y. B., Hong, L. B., Ma, L. & Ma, Q. 2016*a*. Petrogenesis and geochemistry of the Late Carboniferous rear-arc (or back-arc) pillow basaltic lava in the Bogda Mountains, Chinese North Tianshan. *Lithos* **244**, 30–42.

Xie, W., Xu, Y. G., Chen, Y. B., Luo, Z. Y., Hong, L. B., Ma, L. & Liu, H. Q. 2016*b*. High-alumina basalts from the Bogda Mountains suggest an arc setting for Chinese Northern Tianshan during the Late Carboniferous. *Lithos* **256–257**, 165–81.

Xiong, F. H., Yang, J. S., Jia, Y., Xu, X. Z., Chen, S. Y., Li, T. F., Ren, Y. F. & Zuo, G. C. 2011. The pillow lava of Baiyanggou in Bogda, Xinjiang: geochemical and Sr–Nd–Pb isotopic characteristics. *Geology in China* **38**, 838–54 (in Chinese with English abstract).

Xu, X. Y., Li, X. M., Ma, Z. P., Xia, L. Q., Xia, Z. C. & Peng, S. X. 2006. LA-ICP-MS zircon U–Pb dating of gabbro from the Bayingou ophiolite in the Northern Tianshan Mountains. *Acta Geologica Sinica* **80**, 1168–76 (in Chinese with English abstract).

Xu, X. Y., Ma, Z. P., Xia, L. Q., Wang, Y. B., Li, X. M., Xia, Z. C. & Wang, L. S. 2005. SHRIMP dating of the plagiogranite from Bayingou ophiolite in the Northern Tianshan Mountains. *Geological Review* **51**, 523–7 (in Chinese with English abstract).

Yang, W., Jolivet, M., Dupont-Nivet, G., Guo, Z. J., Zhang, Z. C. & Wu, C. D. 2012*a*. Source to sink relations between the Tian Shan and Junggar Basin (northwest China) from Late Palaeozoic to Quaternary: evidence from detrital U–Pb zircon geochronology. *Basin Research* **24**, 1–22.

Yang, T. N., Li, J. Y., Sun, G. H. & Wang, Y. B. 2006. Earlier Devonian active continental arc in Central Tianshan: evidence of geochemical analyses and zircon SHRIMP dating on mylonitized granitic rock. *Acta Petrologica Sinica* **22**, 41–8 (in Chinese with English abstract).

Yang, M., Wang, J. L., wang, J. Q. & Dang, P. F. 2012*b*. Studies on geochemistry, zircon U–Pb geochronology and Hf isotopes of granite in Wangfeng area at the northern margin of Middle Tianshan, Xinjiang. *Acta Petrologica Sinica* **28**, 2121–31 (in Chinese with English abstract).

Yang, G. H., Zhang, W. B., Guo, Y. F., Fu, M. Q., Si, G. H., Su, H. P., Wang, J. F. & Chen, X. H. 2014. LA-ICP-MS zircon U–Pb chronology and geological implications of Sikeshu stitching pluton in the North Tianshan Suture Zone, Xinjiang. *Northwestern Geology* **47**, 83–98 (in Chinese with English abstract).

Yuan, H. L., Gao, S., Liu, X. M., Li, H. M., Günther, D. & Wu, F. Z. 2004. Accurate U–Pb age and trace element determinations of zircon by laser ablation inductively coupled plasma mass spectrometry. *Geostandards Newsletter* **28**, 353–70.

Zhang, C. H., Liu, D. B., Zhang, C. L., Wang, Z. Q. & Yu, Q. X. 2005. Stratigraphic constraints on the initial uplift age of Bogda Shan, Xinjiang, northwest China. *Earth Science Frontiers* **12**, 294–302 (in Chinese with English abstract).

Zhao, T. Y., Xu, S. Q., Zhu, Z. X., Liu, X. & Chen, C. 2014. Geological and geochemical features of Carboniferous volcanic rocks in Bogda–Harlik Mountains, Xinjiang and their tectonic significances. *Geological Review* **69**, 115–24 (in Chinese with English abstract).

Zhou, T. S., Li, P. X., Yang, J. D., Hou, J. P., Liu, S. W., Cheng, Z. W., Wu, S. Z. & Li, Y. A. 1997. Strato-type section of non-marine Permian–Triassic boundary in China. *Xinjiang Geology* **15**, 211–26 (in Chinese with English abstract).

Zhu, Z. X., Li, J. Y., Dong, L. H., Zhang, X. F., Hu, J. W. & Wang, K. Z. 2008. The age determination of Late Carboniferous intrusions in Mangqisu region and its

constraints on the closure of oceanic basin in South Tianshan, Xinjiang. *Acta Petrologica Sinica* **24**, 2761–6 (in Chinese with English abstract).

Zhu, Y. F. & Song, B. 2006. Petrology and SHRIMP chronology of mylonitized Tianger granite, Xinjiang: also about the dating on hydrothermal zircon rim in granite. *Acta Petrologica Sinica* **22**, 135–44 (in Chinese with English abstract).

Zhu, Z. X., Wang, K. Z., Xu, D., Su, Y. L., Wu, Y. L. & Wu, Y. M. 2006. SHRIMP U–Pb dating of zircons from Carboniferous intrusive rocks on the active continental margin of Eren Habirga, West Tianshan, Xinjiang, China, and its geological implications. *Geological Bulletin of China* **25**, 986–91 (in Chinese with English abstract).

Zhu, Y. F., Zhang, L. F., Gu, L. B., Guo, X. & Zhou, J. 2005. Study on trace elements geochemistry and SHRIMP chronology of Carboniferous lava, West Tianshan. *Chinese Science Bulletin* **50**, 2201–12 (in Chinese with English abstract).

https://doi.org/10.1017/S0016756816001217 Published online by Cambridge University Press